

# Use of $W$ -boson longitudinal–transverse interference in top quark spin-correlation functions: II

C.A. Nelson<sup>a</sup>, J.J. Berger, J.R. Wickman

Department of Physics, State University of New York at Binghamton, Binghamton, NY 13902, USA

Received: 27 October 2005 /

Published online: 14 March 2006 – © Springer-Verlag / Società Italiana di Fisica 2006

**Abstract.** This continuation of the derivation of general beam-referenced stage-two spin-correlation functions is for the analysis of top–antitop pair-production at the Tevatron and at the Large Hadron Collider. Both the gluon-production and the quark-production contributions are included for the charged-lepton-plus-jets reaction  $pp$  or  $p\bar{p} \rightarrow t\bar{t} \rightarrow (W^+b)(W^-\bar{b}) \rightarrow (l^+\nu b)(W^-\bar{b})$ . There is a simple 4-angle beam-referenced spin-correlation function for determination of the relative sign of or for measurement of a possible non-trivial phase between the two dominant  $\lambda_b = -1/2$  helicity amplitudes for the  $t \rightarrow W^+b$  decay mode. There is an analogous function and tests for  $\bar{t} \rightarrow W^-\bar{b}$  decay. This signature requires use of the  $(t\bar{t})_{\text{c.m.}}$  energy of the hadronically decaying  $W$ -boson, or the kinematically equivalent cosine of the polar angle of  $W^\mp$  emission in the antitop (top) decay frame. Spinors and their outer-products are constructed so that the helicity-amplitude phase convention of Jacob and Wick can be used throughout for the fixing of the signs associated with this large  $W$ -boson longitudinal–transverse interference effect.

## 1 Introduction: $W$ -boson longitudinal–transverse interference

This continuation of a previous paper [1] on the derivation of general beam-referenced stage-two spin-correlation functions is for the analysis of top–antitop pair production [2, 3] at the Tevatron and at the Large Hadron Collider [4]. Each second at the Large Hadron Collider there will be a top–antitop pair produced when the planned  $L \sim 10^{33} \text{ cm}^{-2}\text{s}^{-1}$  is reached. This should provide an almost ideal “laboratory” for both investigating top-quark physics itself, and for simultaneously improved empirical mastery of reaction backgrounds and detector systematics/performance.

As in the previous paper, which we denote as “I”, the helicity formalism [5] is used for a simple and transparent treatment of all relative phase effects. We use this formalism for investigating the large effects of  $W$ -boson longitudinal–transverse interference in top–antitop pair-production for the charged-lepton plus jets channel, the di-lepton plus jets channel, and the all-jets channel. In “I”, only the quark-production contribution was included; it is the dominant contribution at the Tevatron. On the other hand at the Large Hadron Collider, the gluon-production contribution dominates. To leading order in  $\alpha_s$ , both contributions are included in the analysis in the present paper. The modular property of the helicity-formalism with respect to incorporation of the various density matrices and symmetries again remains manifest throughout this

analysis. This modularity should be easy to exploit in understanding and checking large interference effects in applications of these results.

Using the spinor outer-product formulas obtained in Appendix A, the associated gluon production density-matrix elements are derived in Appendix B in the helicity-amplitude phase convention of Jacob and Wick (JW). The analogous quark-production density-matrix elements were obtained in “I”. They also follow from these spinor outer-products. Besides their dependence on  $\cos \Theta_B$ , these gluon and quark density-matrix elements  $\rho_{\lambda_1 \lambda_2, \lambda'_1 \lambda'_2}(\Theta_B, \Phi_B)$  exhibit several non-trivial overall minus signs and an explicit dependence on the azimuthal angle  $\Phi_B$ . These important spherical angles  $\Theta_B$  and  $\Phi_B$  are defined in Figs. 1 and 2. Otherwise, to avoid repetition, we assume that the reader has “I” available with its figures, discussions, and the sequential-decay density matrices  $R_{\lambda_1 \lambda'_1}(t \rightarrow W^+b \rightarrow (l^+\nu)b)$  and  $\bar{R}_{\lambda_2 \lambda'_2}(\bar{t} \rightarrow W^-\bar{b} \rightarrow (l^-\bar{\nu})\bar{b})$  for the  $CP$ -conjugate process. For the sequential-decay with the first-stage  $t \rightarrow W^+b$  followed by the second-stage  $W^+ \rightarrow l^+\nu$ , the spherical angles  $\theta_a, \phi_a$  specify the  $l^+$  momentum in the  $W_1^+$  rest frame when there is first a boost from the  $(t\bar{t})_{\text{c.m.}}$  frame to the  $t_1$  rest frame, and then a second boost from the  $t_1$  rest frame to the  $W_1^+$  rest frame (see “I”). The  $0^\circ$  direction for the azimuthal angle  $\phi_a$  is defined by the projection of the  $W_2^-$  momentum direction. Analogously, the spherical angles  $\theta_b, \phi_b$  specify the  $l^-$  momentum in the  $W_2^-$  rest frame.

As in “I”, the emphasis is on tests for the charged-lepton-plus-jets reaction  $pp$  or  $p\bar{p} \rightarrow t\bar{t} \rightarrow (W^+b)(W^-\bar{b}) \rightarrow$

<sup>a</sup> e-mail: cnelson@binghamton.edu

$(l^+\nu b)(W^-\bar{b})$ . However, in contrast with the analysis in “I”, because of the differences in dependence on  $\cos\Theta_B$  among the five sets of gluon-production density-matrix elements, for clarity  $\cos\Theta_B$  is not integrated out in the present paper. Consequently, versus the 3-angle stage-two spin-correlation function  $\mathcal{F}|_0 + \mathcal{F}|_{\text{sig}}$  in “I” which only included the quark-production contribution, there is instead a simple 4-angle beam-referenced stage-two spin-correlation function  $\mathcal{G}^{(g,q)}|_0 + \mathcal{G}^{(g,q)}|_{\text{sig}}$  with both gluon (see (2) and (3)) and quark (see (9) and (10)) production contributions.

This BR-S2SC function can be used for the determination of the relative sign of or for measurement of a possible non-trivial phase between the two dominant  $\lambda_b = -1/2$  helicity amplitudes for the  $t \rightarrow W^+b$  decay mode. Both in the SM and in the case of an additional large  $t_R \rightarrow b_L$  chiral weak-transition moment [6], the  $\lambda_b = -1/2$  and  $\lambda_{\bar{b}} = 1/2$  amplitudes are more than  $\sim 30$  times larger than the  $\lambda_b = 1/2$  and  $\lambda_{\bar{b}} = -1/2$  amplitudes. For the  $CP$ -conjugate case, there are analogous tests for  $\bar{t} \rightarrow W^-b$  decay based on the analogous function; see (21) and (22), and (24) and (25).

As in “I”, this important signature from  $W$ -boson longitudinal–transverse interference requires use of the  $(t\bar{t})_{\text{c.m.}}$  energy of the hadronically decaying  $W$ -boson, or the kinematically equivalent cosine of the polar angle of  $W^\mp$  emission in the antitop (top) decay frame,  $\cos\theta_{2,1}^t$ . In application, for instance to  $pp \rightarrow t\bar{t}X$ , parton-level top-quark spin-correlation functions [7, 8] need to be smeared with the appropriate parton distribution functions with integrations over  $\cos\Theta_B$  and the  $(t\bar{t})_{\text{c.m.}}$  energy,  $\sqrt{s}$ . The color factors have been included in these BR-S2SC functions.

For the gluon-production-decay sequence

$$g_1 g_2 \rightarrow t_1 \bar{t}_2 \rightarrow (W^+b)(W^-\bar{b}) \rightarrow \dots, \quad (1)$$

we assume that the  $\lambda_b = -1/2$  and  $\lambda_{\bar{b}} = 1/2$  amplitudes dominate in  $t_1$  and  $\bar{t}_2$  decay. The simple four-angle distribution  $\mathcal{G}^g|_0 + \mathcal{G}^g|_{\text{sig}}$  for  $t_1 \rightarrow W_1^+b \rightarrow (l^+\nu)b$  involves the angles  $\{\Theta_B; \theta_2^t, \theta_a, \phi_a\}$ , where  $\Theta_B$  is shown in Fig. 1. The other angles are displayed in Figs. 1 and 3 of “I”. The “gluon contribution” is

$$\begin{aligned} \mathcal{G}^g|_0 &= \frac{16\pi^3}{3} c(s, \Theta_B) \tilde{g}_1^g(s, \Theta_B) \\ &\times \left\{ \frac{1}{2} \Gamma(0, 0) \sin^2 \theta_a + \Gamma(-1, -1) \sin^4 \frac{\theta_a}{2} \right\} \\ &\times [\bar{\Gamma}(0, 0) + \bar{\Gamma}(1, 1)], \end{aligned} \quad (2)$$

$$\begin{aligned} \mathcal{G}^g|_{\text{sig}} &= -\frac{4\sqrt{2}\pi^4}{3} c(s, \Theta_B) \tilde{g}_2^g(s, \Theta_B) \cos\theta_2^t \sin\theta_a \sin^2 \frac{\theta_a}{2} \\ &\times \{ \Gamma_R(0, -1) \cos\phi_a - \Gamma_I(0, -1) \sin\phi_a \} \\ &\times [\bar{\Gamma}(0, 0) + \bar{\Gamma}(1, 1)] \mathcal{R}, \end{aligned} \quad (3)$$

with two gluon-beam-referencing factors

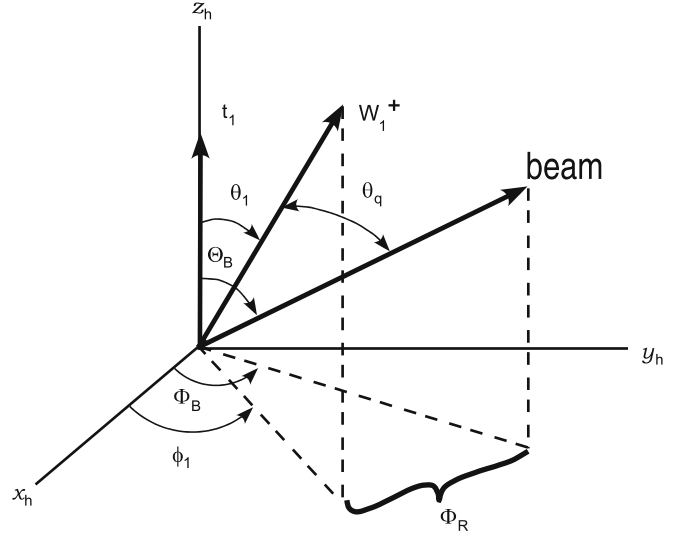


**Fig. 1.** The derivation of the general “beam referenced stage-two-spin-correlation” function begins in the “home” or starting coordinate system  $(x_h, y_h, z_h)$  in the  $(t\bar{t})_{\text{c.m.}}$  frame. The top quark  $t_1$  is moving in the positive  $z_h$  direction, and  $\theta_1, \phi_1$  specify the  $W_1^+$  momentum direction. The  $g_1$  gluon-momentum or  $q_1$  quark-momentum “beam” direction is specified by the spherical angles  $\Theta_B, \Phi_B$ . Note that  $\Phi_R = \Phi_B - \phi_1$

$$\begin{aligned} \tilde{g}_1^g(s, \Theta_B) &= \sin^2 \Theta_B (1 + \cos^2 \Theta_B) \\ &+ \frac{8m^2}{s} (\cos^2 \Theta_B + \sin^4 \Theta_B) \\ &- \frac{16m^4}{s^2} (1 + \sin^4 \Theta_B), \end{aligned} \quad (4)$$

$$\begin{aligned} \tilde{g}_2^g(s, \Theta_B) &= \sin^2 \Theta_B (1 + \cos^2 \Theta_B) \\ &- \frac{8m^2}{s} (1 + \sin^2 \Theta_B) \\ &+ \frac{16m^4}{s^2} (1 + \sin^4 \Theta_B). \end{aligned} \quad (5)$$

The tildes denote the fact that these two factors first appear in the slightly more general five-angle BR-S2SC functions in Sect. 2 in which the  $(t\bar{t})_{\text{c.m.}}$  energy of the leptonically decaying  $W^+$  has not been integrated out, i.e. in which the  $\cos\theta_1^t$  dependence has not been integrated out. The overall pole factor

$$c(s, \Theta_B) = \frac{s^2 g^4}{96(m^2 - t)^2 (m^2 - u)^2} \left[ 7 + \frac{36p^2}{s} \cos^2 \Theta_B \right] \quad (6)$$

depends on the  $(t\bar{t})_{\text{c.m.}}$  center-of-momentum energy  $\sqrt{s}$  and  $\cos\Theta_B$ , and includes the gluon color factor. The “signal” contribution is suppressed by

$$\mathcal{R} \equiv \frac{[\bar{\Gamma}(0, 0) - \bar{\Gamma}(1, 1)]}{[\bar{\Gamma}(0, 0) + \bar{\Gamma}(1, 1)]} \quad (7)$$

which is associated with the stage-one part of the sequential decay  $\bar{t} \rightarrow W^-\bar{b}$ . There is similarly a suppression factor  $\bar{\mathcal{R}}$ , see (23), for the  $CP$ -conjugate channel  $\bar{t}_2 \rightarrow W_2^-\bar{b} \rightarrow$

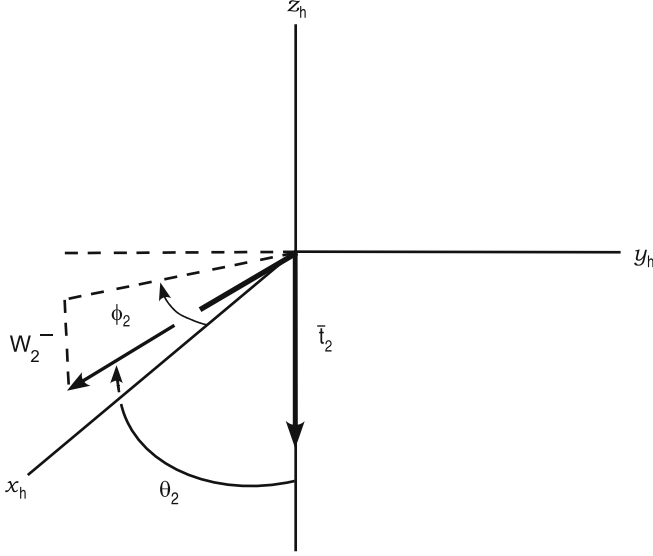


**Fig. 2.** Supplement to previous figure to show  $\theta_2, \phi_2$  which specify the  $W_2^-$  momentum direction. The azimuthal angles  $\phi_1$  and  $\phi_2$  are Lorentz invariant under boosts along the  $z_h$  axis. Note that the sum  $\phi = \phi_1 + \phi_2$  is the angle between the  $t_1$  and  $\bar{t}_2$  decay planes, and that the  $\bar{t}_2$  momentum is in the negative  $z_h$  direction. The three angles  $\theta_1^t, \theta_2^t$  and  $\phi$  describe the first stage in the sequential-decays of the  $t\bar{t}$  system in which  $t_1 \rightarrow W_1^+ b$  and  $\bar{t}_2 \rightarrow W_2^- \bar{b}$ . The angles  $\theta_1^t, \theta_2^t$  are defined respectively in the  $t_1, \bar{t}_2$  rest frames [1]

$(l^- \bar{\nu}) \bar{b}$ . Numerically,  $\mathcal{R} = \overline{\mathcal{R}} = \left(1 - \frac{2m_W^2}{m_t^2}\right) / \left(1 + \frac{2m_W^2}{m_t^2}\right) \sim 0.41$  in both the standard model and in the case of an additional large  $t_R \rightarrow b_L$  chiral weak-transition moment.

For  $g_1(q)g_2(r) \rightarrow t_1(p)\bar{t}_2(l)$ , in terms of the particles' external momenta, useful kinematic formulas are  $s = (q+r)^2 = (p+l)^2 = 4E^2$ ,  $t = (p-q)^2 = (r-l)^2 = m^2 - 2E^2(1 - \beta \cos \Theta_B)$ , and  $u = (p-r)^2 = (q-l)^2 = m^2 - 2E^2(1 + \beta \cos \Theta_B)$  where  $\beta = p/E, \gamma = E/m$  with  $m, E, p$  the top-quark mass, energy, and magnitude of 3-momentum in the  $(t\bar{t})_{\text{c.m.}}$  frame.

For the quark-production-decay sequence

$$q_1 \bar{q}_2 \rightarrow t_1 \bar{t}_2 \rightarrow (W^+ b)(W^- \bar{b}) \rightarrow \dots, \quad (8)$$

we also assume that the  $\lambda_b = -1/2$  and  $\lambda_{\bar{b}} = 1/2$  amplitudes dominate in  $t_1$  and  $\bar{t}_2$  decay. Including the color factor, the four-angle distribution  $\mathcal{G}^q|_0 + \mathcal{G}^q|_{\text{sig}}$  for  $t_1 \rightarrow W_1^+ b \rightarrow (l^+ \nu)b$  or “quark contribution” is

$$\begin{aligned} \mathcal{G}^q|_0 &= \frac{2\pi^3 g^4}{27s^2} \tilde{g}_1^q(s, \Theta_B) \\ &\times \left\{ \frac{1}{2} \Gamma(0, 0) \sin^2 \theta_a + \Gamma(-1, -1) \sin^4 \frac{\theta_a}{2} \right\} \\ &\times [\overline{\Gamma}(0, 0) + \overline{\Gamma}(1, 1)], \quad (9) \\ \mathcal{G}^q|_{\text{sig}} &= -\frac{\sqrt{2}\pi^4 g^4}{54s^2} \tilde{g}_2^q(s, \Theta_B) \cos \theta_2^t \sin \theta_a \sin^2 \frac{\theta_a}{2} \\ &\times \{ \Gamma_R(0, -1) \cos \phi_a - \Gamma_I(0, -1) \sin \phi_a \} \\ &\times [\overline{\Gamma}(0, 0) + \overline{\Gamma}(1, 1)] \mathcal{R}, \quad (10) \end{aligned}$$

with two quark-beam-referencing factors

$$\tilde{g}_1^q(s, \Theta_B) = 1 + \cos^2 \Theta_B + \frac{4m^2}{s} \sin^2 \Theta_B, \quad (11)$$

$$\tilde{g}_2^q(s, \Theta_B) = 1 + \cos^2 \Theta_B - \frac{4m^2}{s} \sin^2 \Theta_B. \quad (12)$$

In terms of the  $t \rightarrow W^+ b$  helicity amplitudes  $A(\lambda_{W^+}, \lambda_b)$  in the  $t_1$  rest frame, the decay density matrix element

$$\begin{aligned} \langle \theta_1^t, \phi_1, \lambda_{W^+}, \lambda_b | \frac{1}{2}, \lambda_1 \rangle &= D_{\lambda_1, \mu}^{(1/2)*}(\phi_1, \theta_1^t, 0) A(\lambda_{W^+}, \lambda_b), \\ A(\lambda_{W^+}, \lambda_b) &\equiv |A(\lambda_{W^+}, \lambda_b)| \exp(i \varphi_{\lambda_{W^+}, \lambda_b}), \end{aligned} \quad (13)$$

where  $\mu = \lambda_{W^+} - \lambda_b$  in terms of the  $W_1^+$  and  $b$ -quark helicities. The dominant polarized-partial widths are

$$\Gamma(0, 0) \equiv |A(0, -1/2)|^2, \quad \Gamma(-1, -1) \equiv |A(-1, -1/2)|^2 \quad (14)$$

and the  $W$ -boson-LT-interference widths are

$$\begin{aligned} \Gamma_R(0, -1) &= \Gamma_R(-1, 0) \equiv \text{Re}[A(0, -1/2)A(-1, -1/2)^*] \\ &\equiv |A(0, -1/2)||A(-1, -1/2)| \cos \beta_L, \quad (15) \end{aligned}$$

$$\begin{aligned} \Gamma_I(0, -1) &= -\Gamma_I(-1, 0) \equiv \text{Im}[A(0, -1/2)A(-1, -1/2)^*] \\ &\equiv -|A(0, -1/2)||A(-1, -1/2)| \sin \beta_L, \quad (16) \end{aligned}$$

where  $\beta_L \equiv \varphi_{-1, -\frac{1}{2}} - \varphi_{0, -\frac{1}{2}}$ .

For the  $CP$ -conjugate process,  $\bar{t}_2 \rightarrow W_2^- \bar{b}$ , in the  $\bar{t}_2$  rest frame, the helicity amplitudes  $B(\lambda_{W^-}, \lambda_{\bar{b}})$  are defined by

$$\begin{aligned} \langle \theta_2^t, \phi_2, \lambda_{W^-}, \lambda_{\bar{b}} | \frac{1}{2}, \lambda_2 \rangle &= D_{\lambda_2, \bar{\mu}}^{(1/2)*}(\phi_2, \theta_2^t, 0) B(\lambda_{W^-}, \lambda_{\bar{b}}), \\ B(\lambda_{W^-}, \lambda_{\bar{b}}) &\equiv |B(\lambda_{W^-}, \lambda_{\bar{b}})| \exp(i \bar{\varphi}_{\lambda_{W^-}, \lambda_{\bar{b}}}), \end{aligned} \quad (17)$$

with  $\bar{\mu} = \lambda_{W^-} - \lambda_{\bar{b}}$ , and

$$\overline{\Gamma}(0, 0) \equiv |B(0, 1/2)|^2, \quad \overline{\Gamma}(1, 1) \equiv |B(1, 1/2)|^2, \quad (18)$$

$$\begin{aligned} \overline{\Gamma}_R(0, 1) &= \overline{\Gamma}_R(1, 0) \equiv \text{Re}[B(0, 1/2)B(1, 1/2)^*] \\ &\equiv |B(0, 1/2)||B(1, 1/2)| \cos \bar{\beta}_R, \quad (19) \end{aligned}$$

$$\begin{aligned} \overline{\Gamma}_I(0, 1) &= -\overline{\Gamma}_I(1, 0) \equiv \text{Im}[B(0, 1/2)B(1, 1/2)^*] \\ &\equiv -|B(0, 1/2)||B(1, 1/2)| \sin \bar{\beta}_R, \quad (20) \end{aligned}$$

where  $\bar{\beta}_R \equiv \bar{\varphi}_{1, \frac{1}{2}} - \bar{\varphi}_{0, \frac{1}{2}}$ .

For the  $CP$ -conjugate channel  $\bar{t}_2 \rightarrow W_2^- \bar{b} \rightarrow (l^- \bar{\nu}) \bar{b}$ , the analogous four-angle BR-S2SC function  $\overline{\mathcal{G}}^g|_0 + \overline{\mathcal{G}}^g|_{\text{sig}}$  is a distribution versus  $\{\Theta_B; \theta_b^t, \theta_b, \phi_b\}$ , where the latter three angles are displayed in Figs. 2 and 3 of “I”. The gluon contribution is

$$\begin{aligned} \overline{\mathcal{G}}^g|_0 &= \frac{16\pi^3}{3} c(s, \Theta_B) \tilde{g}_1^g(s, \Theta_B) \\ &\times \left\{ \frac{1}{2} \overline{\Gamma}(0, 0) \sin^2 \theta_b + \overline{\Gamma}(1, 1) \sin^4 \frac{\theta_b}{2} \right\} \\ &\times [\Gamma(0, 0) + \Gamma(-1, -1)], \quad (21) \end{aligned}$$

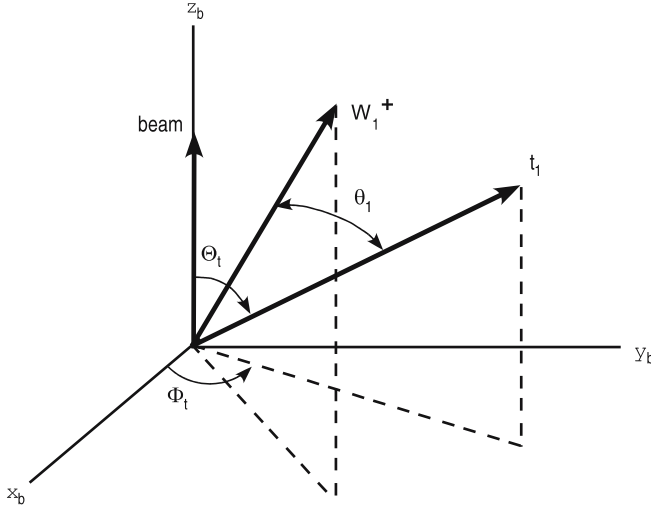


**Fig. 3.** For a derivation of the alternative  $\Theta_t, \Phi_t$  beam-referenced production density-matrix elements, a supplement to Fig.1 to show the  $\Theta_t$  and  $\Phi_t$  angles in the beam coordinate system  $(x_b, y_b, z_b)$  in the  $(t\bar{t})_{\text{c.m.}}$  frame. The  $g_1$  gluon-momentum or  $q_1$  quark-momentum “beam” direction is in the positive  $z_b$  direction. The final  $t_1$  momentum is specified by the spherical angles  $\Theta_t, \Phi_t$ , with the  $t_2$  momentum, not shown, back to back with the  $t_1$

$$\begin{aligned} \overline{\mathcal{G}^g}|_{\text{sig}} &= -\frac{4\sqrt{2}\pi^4}{3} c(s, \Theta_B) \tilde{g}_2^g(s, \Theta_B) \cos \theta_1^t \sin \theta_b \sin^2 \frac{\theta_b}{2} \\ &\times \{ \overline{\Gamma}_R(0, 1) \cos \phi_b + \overline{\Gamma}_1(0, 1) \sin \phi_b \} \\ &\times [\Gamma(0, 0) + \Gamma(-1, -1)] \overline{\mathcal{R}}, \end{aligned} \quad (22)$$

where

$$\overline{\mathcal{R}} \equiv \frac{[\Gamma(0, 0) - \Gamma(-1, -1)]}{[\Gamma(0, 0) + \Gamma(-1, -1)]}. \quad (23)$$

The quark contribution is

$$\begin{aligned} \overline{\mathcal{G}^q}|_0 &= \frac{2\pi^3 g^4}{27s^2} \tilde{g}_1^q(s, \Theta_B) \\ &\times \left\{ \frac{1}{2} \overline{\Gamma}(0, 0) \sin^2 \theta_b + \overline{\Gamma}(1, 1) \sin^4 \frac{\theta_b}{2} \right\} \\ &\times [\Gamma(0, 0) + \Gamma(-1, -1)], \end{aligned} \quad (24)$$

$$\begin{aligned} \overline{\mathcal{G}^q}|_{\text{sig}} &= -\frac{\sqrt{2}\pi^4 g^4}{54s^2} \tilde{g}_2^q(s, \Theta_B) \cos \theta_1^t \sin \theta_b \sin^2 \frac{\theta_b}{2} \\ &\times \{ \overline{\Gamma}_R(0, 1) \cos \phi_b + \overline{\Gamma}_1(0, 1) \sin \phi_b \} \\ &\times [\Gamma(0, 0) + \Gamma(-1, -1)] \overline{\mathcal{R}}. \end{aligned} \quad (25)$$

### 1.1 Structure of four-angle BR-S2SC functions

In general, the  $t_1 \bar{t}_2 \rightarrow (W^+ b)(W^- \bar{b}) \rightarrow (l^+ \nu b)(W^- \bar{b})$  decay-structure of the above four-angle BR-S2SC functions is exactly analogous to that of the quark-production three-angle non-beam-referenced S2SC functions in “I”.

The significant difference is the additional dependence on  $\cos \Theta_B$  due to the beam-referencing. Therefore, for gluon-production there are the two gluon-beam-referencing factors  $\tilde{g}_1^g(s, \Theta_B), \tilde{g}_2^g(s, \Theta_B)$  of (4) and (5), and for quark-production the two quark-beam-referencing factors  $\tilde{g}_1^q(s, \Theta_B), \tilde{g}_2^q(s, \Theta_B)$  of (11) and (12). There is a common final-state interference structure in these BR-S2SC functions for the charged-lepton plus jets reaction  $pp$  or  $p\bar{p} \rightarrow t\bar{t} \rightarrow \dots$ . The final-state relative phase effects do not depend on whether the final  $t_1 \bar{t}_2$  system has been produced by gluon or by quark production.

In these four-angle expressions, the signal contributions are again suppressed by the factor  $\mathcal{R} = (\text{prob } W_L) - (\text{prob } W_T)$  as a consequence of the dynamical assumption that the  $\lambda_b = -1/2$  and  $\lambda_{\bar{b}} = 1/2$  amplitudes dominate. From the  $\theta_2^t$  dependence of the integrated diagonal elements of the sequential-decay density matrices  $\overline{R}_{++}^{\bar{b}R}, \overline{R}_{--}^{\bar{b}R}$  for  $\bar{t}_2 \rightarrow W_2^- \bar{b} \rightarrow (l^- \bar{\nu}) \bar{b}$ ,  $\overline{R}_{++}^{\bar{b}R}$  and  $\overline{R}_{--}^{\bar{b}R}$  [see (95) and (96) of “I”], it follows that  $\mathcal{R}$ 's numerator appears in  $\mathcal{G}^{g,q}|_{\text{sig}}$  multiplied by  $\cos \theta_2^t$  and that  $\mathcal{R}$ 's denominator appears in  $\mathcal{G}^{g,q}|_0$  multiplied by one. The off-diagonal  $\overline{R}_{\lambda_2 \lambda_2'}$  elements which describe  $\bar{t}_2$ -helicity interference do not contribute due to the integration over the opening angle  $\phi$  between the  $t_1$  and  $\bar{t}_2$  decay planes. There are the analogous structures in the four-angle  $\overline{\mathcal{G}^{g,q}}|_0 + \overline{\mathcal{G}^{g,q}}|_{\text{sig}}$  functions for the  $CP$ -conjugate tests.

### 1.2 Outline of this paper

For the production-decay sequence  $g_1 g_2 \rightarrow t_1 \bar{t}_2 \rightarrow (W^+ b)(W^- \bar{b}) \rightarrow \dots$ , Sect. 2 of this paper contains the derivation in the  $(t\bar{t})_{\text{c.m.}}$  frame of the gluon-production BR-S2SC functions in the “home” or starting coordinate system  $(x_h, y_h, z_h)$ , which is defined by Figs.1 and 2 with the top-quark  $t_1$  is moving along the positive  $z_h$  direction. Section 2.1 lists the gluon-production  $t_1 \bar{t}_2$  density-matrix elements in this coordinate system with the  $g_1$  gluon-momentum “beam” direction specified by the spherical angles  $\Theta_B, \Phi_B$ . In Sect. 2.2, the gluon contributions to the general BR-S2SC functions  $I_{\lambda_1 \lambda_2; \lambda_1' \lambda_2'}$  are obtained, and in Sect. 2.3 applied to the lepton-plus-jets channel of the  $t\bar{t}$  system, assuming that the  $\lambda_b = -1/2$  and  $\lambda_{\bar{b}} = 1/2$  amplitudes dominate. The above four-angle gluon-production BR-S2SC function  $\mathcal{G}^g|_0 + \mathcal{G}^g|_{\text{sig}}$  is obtained, along with addition-angle generalizations which might be useful empirically. Analogously, in Sect. 3, the quark-production  $t_1 \bar{t}_2$  density-matrix elements for Figs. 1 and 2 are listed with  $q_1$  quark-momentum “beam” direction specified by the spherical angles  $\Theta_B, \Phi_B$ . The analogous BR-S2SC functions are obtained for the case of quark production  $q_1 \bar{q}_2 \rightarrow t_1 \bar{t}_2 \rightarrow (W^+ b)(W^- \bar{b}) \rightarrow \dots$ . Section 4 contains a summary and a discussion. The appendices respectively contain (A) the Dirac spinors and their outer-products  $u(p, \lambda_1) \bar{u}(p, \lambda_1'), \dots$  in the JW phase convention including the  $CPT$  discrete symmetry properties of the spinors, (B) the derivation of the gluon-production density-matrix elements in the JW phase convention for Figs. 1 and 2, and

(C) the alternative  $\Theta_t, \Phi_t$  production density-matrix elements for the alternative beam-reference system defined by Fig. 3, in which the incident parton “beam” specifies the positive  $z_b$  axis.

## 2 Derivation of gluon-production beam-referenced stage-two spin-correlation functions

The general beam-referenced angular distribution in the  $(t\bar{t})_{\text{c.m.}}$  is

$$\begin{aligned} I(\Theta_B, \Phi_B; \theta_1^t, \phi_1; \theta_a, \phi_a; \theta_2^t, \phi_2; \theta_b, \phi_b) & \\ = \sum_{\lambda_1 \lambda_2 \lambda'_1 \lambda'_2} \rho_{\lambda_1 \lambda_2, \lambda'_1 \lambda'_2}^{\text{prod}}(\Theta_B, \Phi_B) & \\ \times R_{\lambda_1 \lambda'_1}(t \rightarrow W^+ b \rightarrow \dots) \bar{R}_{\lambda_2 \lambda'_2}(\bar{t} \rightarrow W^- \bar{b} \rightarrow \dots), & \end{aligned} \quad (26)$$

where the summations are over the  $t_1$  and  $\bar{t}_2$  helicities. The composite decay-density-matrices  $R_{\lambda_1 \lambda'_1}$  for  $t \rightarrow W^+ b \rightarrow \dots$  and  $\bar{R}_{\lambda_2 \lambda'_2}$  for  $\bar{t} \rightarrow W^- \bar{b} \rightarrow \dots$  are given in Sect. 2.1 of “I”. This formula holds for any of the above  $t\bar{t}$  production channels and for either the lepton-plus-jets, the dilepton-plus-jets, or the all-jets  $t\bar{t}$  decay channels.

In the  $(t\bar{t})_{\text{c.m.}}$  frame, see Figs. 1 and 2, the angles  $\Theta_B, \Phi_B$  specify the direction of the incident beam, the  $g_1$  or  $q_1$  momentum. The  $t_1$  momentum is chosen to lie along the positive  $z_h$  axis. The positive  $x_h$  direction is an arbitrary, fixed perpendicular direction. Because the incident beam is assumed to be unpolarized, there is no dependence on the associated  $\phi_1$  angle after the observable azimuthal angles are specified (see below). With respect to the normalization of the various BR-S2SC functions, the  $\phi_1$  integration is not explicitly performed in this paper. With (26) there is an associated differential counting rate

$$\begin{aligned} dN = I(\Theta_B, \Phi_B; \dots) d(\cos \Theta_B) d\Phi_B d(\cos \theta_1^t) d\phi_1 & \\ \times d(\cos \theta_a) d\phi_a d(\cos \theta_2^t) d\phi_2 d(\cos \theta_b) d\phi_b, & \end{aligned} \quad (27)$$

where, for full phase space, the cosine of each polar angle ranges from  $-1$  to  $1$ , and each azimuthal angle ranges over  $2\pi$ .

We use the helicity indices to label the successive terms in the gluon contributions to the sum in (26). Each term is denoted  $I_{\lambda_1 \lambda_2; \lambda'_1 \lambda'_2}^g$  with  $\lambda_1 \lambda_2, \dots$  the signs of the  $t_1, \bar{t}_2$  helicities. Unlike in “I”, in this paper we do not use superscripts “m” and “m2” to emphasize the mixed-helicity and helicity-flip contributions versus the non-superscripted helicity-conserving ones, since a quick glance at the patterns in these subscripted helicity indices provides these distinctions. The charged lepton’s azimuthal angle  $\phi_a$  or  $\phi_b$  is always referenced by the opposite  $W^\mp$ -boson momentum, so these charged-lepton azimuthal angles are denoted

without “tilded accents”. For the alternative  $\widetilde{\phi}_a$  and  $\widetilde{\phi}_b$  referencing by the opposite  $\bar{t}_2, t_1$  momentum directions, see the discussion in 2nd and 3rd paragraphs of Sect. 2 of “I”.

### 2.1 Gluon-production density matrix in Jacob and Wick phase convention

The  $t_1 \bar{t}_2$  helicity-conserving gluon-production density-matrix elements in the  $(t\bar{t})_{\text{c.m.}}$  system are

$$\rho_{+-,+ -}^g = \rho_{-+,- +}^g = c(s, \Theta_B) \frac{4p^2}{s} \sin^2 \Theta_B (1 + \cos^2 \Theta_B), \quad (28)$$

$$\rho_{-+,- +}^g = \{\rho_{+-,+ -}^g\}^* = c(s, \Theta_B) \frac{4p^2}{s} e^{i2\Phi_B} \sin^4 \Theta_B, \quad (29)$$

where the asterisk denotes complex-conjugation, and the common pole factor  $c(E, \Theta_B)$  is given in (6) in the introduction. Note the  $e^{i2\Phi_B}$  factor in (29).

The mixed helicity-properties gluon-production density-matrix elements are

$$\rho_{-+,- +}^g = \rho_{-+,- -}^g = -\rho_{--,- +}^g = -\rho_{++,- +}^g = \quad (30)$$

$$\{\rho_{++,- +}^g\}^* = \{\rho_{--,- +}^g\}^* = -\{\rho_{+-,- -}^g\}^* = -\{\rho_{-+,- +}^g\}^* \quad (31)$$

$$= -c(s, \Theta_B) \frac{8p^2 m}{s^{3/2}} e^{i\Phi_B} \sin^3 \Theta_B \cos \Theta_B, \quad (32)$$

with an overall minus sign and  $e^{i\Phi_B}$  factor.

The helicity-flip gluon-production density-matrix-elements are

$$\begin{aligned} \rho_{++,- +}^g &= \rho_{--,- -}^g \\ &= c(s, \Theta_B) \frac{4m^2}{s} \left(1 + \frac{4p^2}{s} [1 + \sin^4 \Theta_B]\right), \end{aligned} \quad (33)$$

$$\begin{aligned} \rho_{++,- -}^g &= \rho_{--,- +}^g \\ &= c(s, \Theta_B) \frac{4m^2}{s} \left(1 - \frac{4p^2}{s} [1 + \sin^4 \Theta_B]\right). \end{aligned} \quad (34)$$

### 2.2 Gluon contributions to BR-S2SC function

The helicity-conserving contribution is

$$I_{+-,+ -}^g = \frac{4p^2}{s} c(s, \Theta_B) R_{++} \bar{R}_{--} \sin^2 \Theta_B (1 + \cos^2 \Theta_B), \quad (35)$$

$$I_{-+,- +}^g = \frac{4p^2}{s} c(s, \Theta_B) R_{--} \bar{R}_{++} \sin^2 \Theta_B (1 + \cos^2 \Theta_B), \quad (36)$$

$$I_{+-,- +}^g = \frac{4p^2}{s} c(s, \Theta_B) e^{-i(2\Phi_R + \phi)} r_{+-} \bar{r}_{-+} \sin^4 \Theta_B, \quad (37)$$

$$I_{-+,- +}^g = \frac{4p^2}{s} c(s, \Theta_B) e^{i(2\Phi_R + \phi)} r_{-+} \bar{r}_{+-} \sin^4 \Theta_B, \quad (38)$$

where  $R_{++}$ ,  $R_{--}$ ,  $\bar{R}_{++}$ ,  $\bar{R}_{--}$ , are the diagonal elements, and  $(r_{-+})^* = r_{+-} = F_a + iH_a$ ,  $(\bar{r}_{-+})^* = \bar{r}_{+-} = -F_b - iH_b$  the off-diagonal elements of the sequential-decay density matrices  $R_{\lambda_1\lambda_1'}(t \rightarrow W^+b \rightarrow (l^+\nu)b)$  and  $\bar{R}_{\lambda_2\lambda_2'}(\bar{t} \rightarrow W^-\bar{b} \rightarrow (l^-\bar{\nu})\bar{b})$ . As in Sect. 2.2.1 of “I”, in the  $I^g_{\lambda_1\lambda_2,\lambda_1'\lambda_2'}$  and  $I^q_{\lambda_1\lambda_2,\lambda_1'\lambda_2'}$  contributions in this paper, the starting angles  $\phi_2$  and  $\Phi_B$  have been replaced by the angles  $\phi = \phi_1 + \phi_2$  and  $\Phi_R = \Phi_B - \phi_1$ .

The first part of the mixed helicity-properties contribution is

$$I^g_{++,-} = -\frac{8p^2m}{s^{3/2}} c(s, \Theta_B) R_{++}(F_b + iH_b) \sin^3 \Theta_B \times \cos \Theta_B e^{i(\Phi_R + \phi)}, \quad (39)$$

$$I^g_{--,-} = \frac{8p^2m}{s^{3/2}} c(s, \Theta_B) R_{--}(F_b - iH_b) \sin^3 \Theta_B \times \cos \Theta_B e^{-i(\Phi_R + \phi)}, \quad (40)$$

$$I^g_{+-,-} = -\frac{8p^2m}{s^{3/2}} c(s, \Theta_B) (F_a + iH_a) \bar{R}_{++} \sin^3 \Theta_B \times \cos \Theta_B e^{-i\Phi_R}, \quad (41)$$

$$I^g_{-+,-} = \frac{8p^2m}{s^{3/2}} c(s, \Theta_B) (F_a - iH_a) \bar{R}_{--} \sin^3 \Theta_B \times \cos \Theta_B e^{i\Phi_R}. \quad (42)$$

The second part of the mixed helicity-properties contribution is

$$I^g_{+-,+} = -\frac{8p^2m}{s^{3/2}} c(s, \Theta_B) R_{++}(F_b - iH_b) \sin^3 \Theta_B \times \cos \Theta_B e^{-i(\Phi_R + \phi)}, \quad (43)$$

$$I^g_{-+,-} = \frac{8p^2m}{s^{3/2}} c(s, \Theta_B) R_{--}(F_b + iH_b) \sin^3 \Theta_B \times \cos \Theta_B e^{i(\Phi_R + \phi)}, \quad (44)$$

$$I^g_{+-,-} = \frac{8p^2m}{s^{3/2}} c(s, \Theta_B) (F_a + iH_a) \bar{R}_{--} \sin^3 \Theta_B \times \cos \Theta_B e^{-i\Phi_R}, \quad (45)$$

$$I^g_{-+,-} = -\frac{8p^2m}{s^{3/2}} c(s, \Theta_B) (F_a - iH_a) \bar{R}_{++} \sin^3 \Theta_B \times \cos \Theta_B e^{i\Phi_R}. \quad (46)$$

The helicity-flip contribution is

$$I^g_{++,+} = \frac{4m^2}{s} c(s, \Theta_B) R_{++} \bar{R}_{++} \left[ 1 + \frac{4p^2}{s} (1 + \sin^4 \Theta_B) \right], \quad (47)$$

$$I^g_{--,-} = \frac{4m^2}{s} c(s, \Theta_B) R_{--} \bar{R}_{--} \left[ 1 + \frac{4p^2}{s} (1 + \sin^4 \Theta_B) \right], \quad (48)$$

$$I^g_{+-,-} = \frac{4m^2}{s} c(s, \Theta_B) e^{i\phi} r_{+-} \bar{r}_{+-} \times \left[ 1 - \frac{4p^2}{s} (1 + \sin^4 \Theta_B) \right], \quad (49)$$

$$I^g_{-+,-} = \frac{4m^2}{s} c(s, \Theta_B) e^{-i\phi} r_{-+} \bar{r}_{-+} \times \left[ 1 - \frac{4p^2}{s} (1 + \sin^4 \Theta_B) \right]. \quad (50)$$

### 2.3 Lepton-plus-jets channel: $\lambda_b = -1/2$ , $\lambda_{\bar{b}} = +1/2$ dominance

From the perspective of specific  $t\bar{t}$  decay channels and/or specific helicity amplitude tests, one can use the above results to investigate various BR-S2SC functions. For instance, in this paper, we are most interested in the “lepton-plus-jets channel” and in tests for the relative sign of or for measurement of a possible non-trivial phase between the  $\lambda_b = -1/2$  helicity amplitudes for  $t \rightarrow W^+b$ . We assume that the  $\lambda_b = -1/2$  and  $\lambda_{\bar{b}} = 1/2$  contributions dominate.

#### 2.3.1 $t_1 \rightarrow W_1^+b \rightarrow (l^+\nu)b$

For the case  $t_1 \rightarrow W_1^+b \rightarrow (l^+\nu)b$ , with  $W_2^-$  decaying into hadronic jets, we separate the intensity contributions into two parts: “signal terms”  $\tilde{I}|_{\text{sig}}$  which depend on  $\Gamma_R(0, -1)$  and  $\Gamma_I(0, -1)$ , and “background terms”  $\tilde{I}|_0$  which depend on  $\Gamma(0, 0)$  and  $\Gamma(-1, -1)$ . In this section, we use a tilde accent on  $\tilde{I}|_0, \dots$  to denote the integration over the  $\theta_b, \phi_b$  variables. By (95)–(97) of “I”, this integration directly projects out the various  $\bar{\Gamma}(\lambda_W, \lambda_{W'})$  dependencies.

We find for the helicity-conserving contribution

$$(\tilde{I}_{+-,-}^g + \tilde{I}_{-+,-}^g)|_0 = \frac{8\pi p^2}{3s} c(s, \Theta_B) \sin^2 \Theta_B (1 + \cos^2 \Theta_B) \quad (51)$$

$$\times \left\{ \begin{array}{l} \frac{1}{2} \Gamma(0, 0) \sin^2 \theta_a [\bar{\Gamma}(0, 0) (1 + \cos \theta_1^t \cos \theta_2^t) \\ + \bar{\Gamma}(1, 1) (1 - \cos \theta_1^t \cos \theta_2^t)] \\ + \Gamma(-1, -1) \sin^4 \frac{\theta_a}{2} [\bar{\Gamma}(0, 0) (1 - \cos \theta_1^t \cos \theta_2^t) \\ + \bar{\Gamma}(1, 1) (1 + \cos \theta_1^t \cos \theta_2^t)] \end{array} \right\},$$

$$(\tilde{I}_{+-,-}^g + \tilde{I}_{-+,-}^g)|_{\text{sig}} = \frac{8\sqrt{2}\pi p^2}{3s} c(s, \Theta_B) \sin^2 \Theta_B (1 + \cos^2 \Theta_B) \times \sin \theta_1^t \cos \theta_2^t \sin \theta_a \sin^2 \frac{\theta_a}{2} \times \{-\Gamma_R(0, -1) \cos \phi_a + \Gamma_I(0, -1) \sin \phi_a\} \times [\bar{\Gamma}(0, 0) - \bar{\Gamma}(1, 1)], \quad (52)$$

$$(\tilde{I}_{+-,-}^g + \tilde{I}_{-+,-}^g)|_0 = -\frac{8\pi p^2}{3s} c(s, \Theta_B) \sin^4 \Theta_B \cos(2\Phi_R + \phi) \sin \theta_1^t \sin \theta_2^t \times \left\{ \frac{1}{2} \Gamma(0, 0) \sin^2 \theta_a - \Gamma(-1, -1) \sin^4 \frac{\theta_a}{2} \right\} \times [\bar{\Gamma}(0, 0) - \bar{\Gamma}(1, 1)], \quad (53)$$

$$\begin{aligned}
 & (\tilde{I}_{+-,-,+}^g + \tilde{I}_{-+,-,+}^g)|_{\text{sig}} \\
 &= -\frac{8\sqrt{2}\pi p^2}{3s} c(s, \Theta_B) \sin^4 \Theta_B \sin \theta_2^t \sin \theta_a \sin^2 \frac{\theta_a}{2} \quad (54) \\
 & \times \left\{ \begin{array}{l} \cos(2\Phi_R + \phi) \\ \cos \theta_1^t \{ \Gamma_R(0, -1) \cos \phi_a - \Gamma_I(0, -1) \sin \phi_a \} \\ + \sin(2\Phi_R + \phi) \\ \{ \Gamma_R(0, -1) \sin \phi_a + \Gamma_I(0, -1) \cos \phi_a \} \end{array} \right\} \\
 & \times [\bar{\Gamma}(0, 0) - \bar{\Gamma}(1, 1)].
 \end{aligned}$$

We collect the mixed-helicity contributions in real sums:

$$\begin{aligned}
 & (\tilde{I}_{-+,++}^g + \tilde{I}_{--,+-}^g + \tilde{I}_{+,-,--}^g + \tilde{I}_{++,,-}^g)|_0 \\
 &= \frac{32\pi p^2 m}{3s^{3/2}} c(s, \Theta_B) \sin^3 \Theta_B \cos \Theta_B \quad (55) \\
 & \cos \Phi_R \sin \theta_1^t \cos \theta_2^t \\
 & \times \left\{ \frac{1}{2} \Gamma(0, 0) \sin^2 \theta_a - \Gamma(-1, -1) \sin^4 \frac{\theta_a}{2} \right\} \\
 & \times [\bar{\Gamma}(0, 0) - \bar{\Gamma}(1, 1)],
 \end{aligned}$$

$$\begin{aligned}
 & (\tilde{I}_{-+,++}^g + \tilde{I}_{--,+-}^g + \tilde{I}_{+,-,--}^g + \tilde{I}_{++,,-}^g)|_{\text{sig}} \\
 &= \frac{32\sqrt{2}\pi p^2 m}{3s^{3/2}} c(s, \Theta_B) \sin^3 \Theta_B \cos \Theta_B \quad (56) \\
 & \times \cos \theta_2^t \sin \theta_a \sin^2 \frac{\theta_a}{2} \\
 & \times \left\{ \begin{array}{l} \cos \theta_1^t \{ \Gamma_R(0, -1) \cos \phi_a - \Gamma_I(0, -1) \sin \phi_a \} \cos \Phi_R \\ + \{ \Gamma_R(0, -1) \sin \phi_a + \Gamma_I(0, -1) \cos \phi_a \} \sin \Phi_R \end{array} \right\} \\
 & \times [\bar{\Gamma}(0, 0) - \bar{\Gamma}(1, 1)],
 \end{aligned}$$

$$\begin{aligned}
 & (\tilde{I}_{++,+-}^g + \tilde{I}_{--,,-}^g + \tilde{I}_{+,-,++}^g + \tilde{I}_{-+,-,-}^g)|_0 \\
 &= -\frac{32\pi p^2 m}{3s^{3/2}} c(s, \Theta_B) \sin^3 \Theta_B \cos \Theta_B \quad (57) \\
 & \times \cos(\Phi_R + \phi) \cos \theta_1^t \sin \theta_2^t \\
 & \times \left\{ \frac{1}{2} \Gamma(0, 0) \sin^2 \theta_a - \Gamma(-1, -1) \sin^4 \frac{\theta_a}{2} \right\} \\
 & \times [\bar{\Gamma}(0, 0) - \bar{\Gamma}(1, 1)],
 \end{aligned}$$

$$\begin{aligned}
 & (\tilde{I}_{++,+-}^g + \tilde{I}_{--,,-}^g + \tilde{I}_{+,-,++}^g + \tilde{I}_{-+,-,-}^g)|_{\text{sig}} \\
 &= \frac{32\sqrt{2}\pi p^2 m}{3s^{3/2}} c(s, \Theta_B) \sin^3 \Theta_B \cos \Theta_B \quad (58) \\
 & \times \cos(\Phi_R + \phi) \sin \theta_1^t \sin \theta_2^t \sin \theta_a \sin^2 \frac{\theta_a}{2} \\
 & \times \{ \Gamma_R(0, -1) \cos \phi_a - \Gamma_I(0, -1) \sin \phi_a \} \\
 & \times [\bar{\Gamma}(0, 0) - \bar{\Gamma}(1, 1)].
 \end{aligned}$$

The helicity-flip contributions are

$$\begin{aligned}
 & (\tilde{I}_{++,++}^g + \tilde{I}_{--,--}^g)|_0 \\
 &= \frac{8\pi m^2}{3s} c(s, \Theta_B) \left[ 1 + \frac{4p^2}{s} (1 + \sin^4 \Theta_B) \right] \quad (59)
 \end{aligned}$$

$$\begin{aligned}
 & \times \left\{ \begin{array}{l} \frac{1}{2} \Gamma(0, 0) \sin^2 \theta_a [\bar{\Gamma}(0, 0) (1 - \cos \theta_1^t \cos \theta_2^t) \\ + \bar{\Gamma}(1, 1) (1 + \cos \theta_1^t \cos \theta_2^t)] \\ + \Gamma(-1, -1) \sin^4 \frac{\theta_a}{2} [\bar{\Gamma}(0, 0) (1 + \cos \theta_1^t \cos \theta_2^t) \\ + \bar{\Gamma}(1, 1) (1 - \cos \theta_1^t \cos \theta_2^t)] \end{array} \right\}, \\
 & (\tilde{I}_{++,++}^g + \tilde{I}_{--,--}^g)|_{\text{sig}} \\
 &= \frac{8\sqrt{2}\pi m^2}{3s} c(s, \Theta_B) \left[ 1 + \frac{4p^2}{s} (1 + \sin^4 \Theta_B) \right] \quad (60) \\
 & \times \sin \theta_1^t \cos \theta_2^t \sin \theta_a \sin^2 \frac{\theta_a}{2} \\
 & \times \{ \Gamma_R(0, -1) \cos \phi_a - \Gamma_I(0, -1) \sin \phi_a \} \\
 & \times [\bar{\Gamma}(0, 0) - \bar{\Gamma}(1, 1)],
 \end{aligned}$$

$$\begin{aligned}
 & (\tilde{I}_{++,--}^g + \tilde{I}_{--,++}^g)|_0 \\
 &= \frac{8\pi m^2}{3s} c(s, \Theta_B) \left[ 1 - \frac{4p^2}{s} (1 + \sin^4 \Theta_B) \right] \quad (61) \\
 & \times \cos \phi \sin \theta_1^t \sin \theta_2^t \\
 & \times \left\{ -\frac{1}{2} \Gamma(0, 0) \sin^2 \theta_a + \Gamma(-1, -1) \sin^4 \frac{\theta_a}{2} \right\} \\
 & \times [\bar{\Gamma}(0, 0) - \bar{\Gamma}(1, 1)],
 \end{aligned}$$

$$\begin{aligned}
 & (\tilde{I}_{++,--}^g + \tilde{I}_{--,++}^g)|_{\text{sig}} \\
 &= \frac{8\sqrt{2}\pi m^2}{3s} c(s, \Theta_B) \left[ 1 - \frac{4p^2}{s} (1 + \sin^4 \Theta_B) \right] \sin \theta_2^t \sin \theta_a \quad (62) \\
 & \times \sin^2 \frac{\theta_a}{2} \\
 & \times \left\{ \begin{array}{l} \cos \phi \cos \theta_1^t \{ -\Gamma_R(0, -1) \cos \phi_a + \Gamma_I(0, -1) \sin \phi_a \} \\ + \sin \phi \{ \Gamma_R(0, -1) \sin \phi_a + \Gamma_I(0, -1) \cos \phi_a \} \end{array} \right\} \\
 & \times [\bar{\Gamma}(0, 0) - \bar{\Gamma}(1, 1)].
 \end{aligned}$$

## 2.4 $\bar{t}_2 \rightarrow W_2^- \bar{b} \rightarrow (l^- \bar{\nu}) \bar{b}$

For the  $CP$ -conjugate process  $\bar{t}_2 \rightarrow W_2^- \bar{b} \rightarrow (l^- \bar{\nu}) \bar{b}$ , with  $W_1^+$  decaying into hadronic jets, we similarly separate the contributions: “signal terms”  $\tilde{T}|_{\text{sig}}$  depending on  $\bar{T}_R(0, 1)$  and  $\bar{T}_I(0, 1)$ , and “background terms”  $\tilde{T}|_0$  depending on  $\bar{\Gamma}(0, 0)$  and  $\bar{\Gamma}(1, 1)$ .

By integration over  $\theta_a, \phi_a$ , we find for the helicity-conserving contribution

$$\begin{aligned}
 & (\tilde{T}_{+-,-,+}^g + \tilde{T}_{-+,-,+}^g)|_0 \\
 &= \frac{8\pi p^2}{3s} c(s, \Theta_B) \sin^2 \Theta_B (1 + \cos^2 \Theta_B) \quad (63) \\
 & \times \left\{ \begin{array}{l} \frac{1}{2} \bar{\Gamma}(0, 0) \sin^2 \theta_b [\Gamma(0, 0) (1 + \cos \theta_1^t \cos \theta_2^t) \\ + \Gamma(-1, -1) (1 - \cos \theta_1^t \cos \theta_2^t)] \\ + \bar{\Gamma}(1, 1) \sin^4 \frac{\theta_b}{2} [\Gamma(0, 0) (1 - \cos \theta_1^t \cos \theta_2^t) \\ + \Gamma(-1, -1) (1 + \cos \theta_1^t \cos \theta_2^t)] \end{array} \right\}, \\
 & (\tilde{T}_{+-,-,+}^g + \tilde{T}_{-+,-,+}^g)|_{\text{sig}}
 \end{aligned}$$

$$\begin{aligned}
&= -\frac{8\sqrt{2}\pi p^2}{3s} c(s, \Theta_B) \sin^2 \Theta_B (1 + \cos^2 \Theta_B) \cos \theta_1^t \sin \theta_2^t \\
&\quad \times \sin \theta_b \sin^2 \frac{\theta_b}{2} \left\{ \bar{\Gamma}_R(0, 1) \cos \phi_b + \bar{\Gamma}_I(0, 1) \sin \phi_b \right\} \\
&\quad \times [\Gamma(0, 0) - \Gamma(-1, -1)], \tag{64}
\end{aligned}$$

$$\begin{aligned}
&(\tilde{I}_{+-,-+}^g + \tilde{I}_{-+,-+}^g)|_0 \\
&= -\frac{8\pi p^2}{3s} c(s, \Theta_B) \sin^4 \Theta_B \cos(2\Phi_R + \phi) \sin \theta_1^t \sin \theta_2^t \\
&\quad \times \left\{ \frac{1}{2} \bar{\Gamma}(0, 0) \sin^2 \theta_b - \bar{\Gamma}(1, 1) \sin^4 \frac{\theta_b}{2} \right\} \\
&\quad \times [\Gamma(0, 0) - \Gamma(-1, -1)],
\end{aligned}$$

$$\begin{aligned}
&(\tilde{I}_{+-,-+}^g + \tilde{I}_{-+,-+}^g)|_{\text{sig}} \\
&= -\frac{8\sqrt{2}\pi p^2}{3s} c(s, \Theta_B) \sin^4 \Theta_B \sin \theta_1^t \sin \theta_b \sin^2 \frac{\theta_b}{2} \\
&\quad \times \left\{ \begin{array}{l} \cos(2\Phi_R + \phi) \cos \theta_2^t \\ \times \left\{ \bar{\Gamma}_R(0, 1) \cos \phi_b + \bar{\Gamma}_I(0, 1) \sin \phi_b \right\} \\ - \sin(2\Phi_R + \phi) \\ \times \left\{ \bar{\Gamma}_R(0, 1) \sin \phi_b - \bar{\Gamma}_I(0, 1) \cos \phi_b \right\} \end{array} \right\} \\
&\quad \times [\Gamma(0, 0) - \Gamma(-1, -1)].
\end{aligned}$$

The mixed-helicity contributions are

$$\begin{aligned}
&(\tilde{I}_{-+,++}^g + \tilde{I}_{-+,-+}^g + \tilde{I}_{+-,--}^g + \tilde{I}_{++,+-}^g)|_0 \\
&= \frac{32\pi p^2 m}{3s^{3/2}} c(E, \Theta_B) \sin^3 \Theta_B \cos \Theta_B \\
&\quad \times \cos \Phi_R \sin \theta_1^t \cos \theta_2^t \\
&\quad \times \left\{ \frac{1}{2} \bar{\Gamma}(0, 0) \sin^2 \theta_b - \bar{\Gamma}(1, 1) \sin^4 \frac{\theta_b}{2} \right\} \\
&\quad \times [\Gamma(0, 0) - \Gamma(-1, -1)],
\end{aligned}$$

$$\begin{aligned}
&(\tilde{I}_{-+,++}^g + \tilde{I}_{-+,-+}^g + \tilde{I}_{+-,--}^g + \tilde{I}_{++,+-}^g)|_{\text{sig}} \\
&= -\frac{32\sqrt{2}\pi p^2 m}{3s^{3/2}} c(s, \Theta_B) \sin^3 \Theta_B \cos \Theta_B \\
&\quad \times \cos \Phi_R \sin \theta_1^t \sin \theta_2^t \sin \theta_b \sin^2 \frac{\theta_b}{2} \\
&\quad \times \left\{ \bar{\Gamma}_R(0, 1) \cos \phi_b + \bar{\Gamma}_I(0, 1) \sin \phi_b \right\} \\
&\quad \times [\Gamma(0, 0) - \Gamma(-1, -1)],
\end{aligned}$$

$$\begin{aligned}
&(\tilde{I}_{++,+-}^g + \tilde{I}_{-+,-+}^g + \tilde{I}_{+-,++}^g + \tilde{I}_{-+,-+}^g)|_0 \\
&= -\frac{32\pi p^2 m}{3s^{3/2}} c(s, \Theta_B) \sin^3 \Theta_B \cos \Theta_B \\
&\quad \times \cos(\Phi_R + \phi) \cos \theta_1^t \sin \theta_2^t \\
&\quad \times \left\{ \frac{1}{2} \bar{\Gamma}(0, 0) \sin^2 \theta_b - \bar{\Gamma}(1, 1) \sin^4 \frac{\theta_b}{2} \right\} \\
&\quad \times [\Gamma(0, 0) - \Gamma(-1, -1)],
\end{aligned}$$

$$\begin{aligned}
&(\tilde{I}_{++,+-}^g + \tilde{I}_{-+,-+}^g + \tilde{I}_{+-,++}^g + \tilde{I}_{-+,-+}^g)|_{\text{sig}} \\
&= -\frac{32\sqrt{2}\pi p^2 m}{3s^{3/2}} c(s, \Theta_B) \sin^3 \Theta_B \cos \Theta_B \cos \theta_1^t \tag{70}
\end{aligned}$$

$$\begin{aligned}
&\times \sin \theta_b \sin^2 \frac{\theta_b}{2} \\
&\quad \times \left\{ \begin{array}{l} \cos \theta_2^t \left\{ \bar{\Gamma}_R(0, 1) \cos \phi_b + \bar{\Gamma}_I(0, 1) \sin \phi_b \right\} \\ \times \cos(\Phi_R + \phi) \\ + \left\{ -\bar{\Gamma}_R(0, 1) \sin \phi_b + \bar{\Gamma}_I(0, 1) \cos \phi_b \right\} \\ \times \sin(\Phi_R + \phi) \end{array} \right\} \\
&\quad \times [\Gamma(0, 0) - \Gamma(-1, -1)].
\end{aligned}$$

The helicity-flip contributions are

$$\begin{aligned}
&(\tilde{I}_{++,++}^g + \tilde{I}_{--,--}^g)|_0 \\
&= \frac{8\pi m^2}{3s} c(s, \Theta_B) \left[ 1 + \frac{4p^2}{s} (1 + \sin^4 \Theta_B) \right] \tag{71} \\
&\quad \times \left\{ \begin{array}{l} \frac{1}{2} \bar{\Gamma}(0, 0) \sin^2 \theta_b [\Gamma(0, 0) (1 - \cos \theta_1^t \cos \theta_2^t) \\ + \Gamma(-1, -1) (1 + \cos \theta_1^t \cos \theta_2^t)] \\ + \bar{\Gamma}(1, 1) \sin^4 \frac{\theta_b}{2} [\Gamma(0, 0) (1 + \cos \theta_1^t \cos \theta_2^t) \\ + \Gamma(-1, -1) (1 - \cos \theta_1^t \cos \theta_2^t)] \end{array} \right\},
\end{aligned}$$

$$\begin{aligned}
&(\tilde{I}_{++,++}^g + \tilde{I}_{--,--}^g)|_{\text{sig}} \\
&= \frac{8\sqrt{2}\pi m^2}{3s} c(s, \Theta_B) \left[ 1 + \frac{4p^2}{s} (1 + \sin^4 \Theta_B) \right] \tag{72} \\
&\quad \times \cos \theta_1^t \sin \theta_2^t \sin \theta_b \sin^2 \frac{\theta_b}{2} \\
&\quad \times \left\{ \bar{\Gamma}_R(0, 1) \cos \phi_b + \bar{\Gamma}_I(0, 1) \sin \phi_b \right\} \\
&\quad \times [\Gamma(0, 0) - \Gamma(-1, -1)],
\end{aligned}$$

$$\begin{aligned}
&(\tilde{I}_{++,--}^g + \tilde{I}_{--,++}^g)|_0 \\
&= \frac{8\pi m^2}{3s} c(s, \Theta_B) \left[ 1 - \frac{4p^2}{s} (1 + \sin^4 \Theta_B) \right] \tag{73} \\
&\quad \times \cos \phi \sin \theta_1^t \sin \theta_2^t \\
&\quad \times \left\{ -\frac{1}{2} \bar{\Gamma}(0, 0) \sin^2 \theta_b + \bar{\Gamma}(1, 1) \sin^4 \frac{\theta_b}{2} \right\} \\
&\quad \times [\Gamma(0, 0) - \Gamma(-1, -1)],
\end{aligned}$$

$$\begin{aligned}
&(\tilde{I}_{++,--}^g + \tilde{I}_{--,++}^g)|_{\text{sig}} \\
&= -\frac{8\sqrt{2}\pi m^2}{3s} c(s, \Theta_B) \left[ 1 - \frac{4p^2}{s} (1 + \sin^4 \Theta_B) \right] \sin \theta_1^t \sin \theta_b \\
&\quad \times \sin^2 \frac{\theta_b}{2} \\
&\quad \times \left\{ \begin{array}{l} \cos \phi \cos \theta_2^t \left\{ \bar{\Gamma}_R(0, 1) \cos \phi_b + \bar{\Gamma}_I(0, 1) \sin \phi_b \right\} \\ - \sin \phi \left\{ \bar{\Gamma}_R(0, 1) \sin \phi_b - \bar{\Gamma}_I(0, 1) \cos \phi_b \right\} \end{array} \right\} \\
&\quad \times [\Gamma(0, 0) - \Gamma(-1, -1)]. \tag{74}
\end{aligned}$$

## 2.5 $\Gamma(\lambda_W, \lambda_{W'})$ tests versus angular dependence

In summary, with beam-referencing, for the  $t_1 \rightarrow W_1^+ b \rightarrow (l^+ \nu) b$  case there are six ‘‘background terms’’ depending on  $\Gamma(0, 0)$  and  $\Gamma(-1, -1)$ , and also six ‘‘signal terms’’ depending on  $\Gamma_{R,I}(0, -1)$ . As a consequence of Lorentz invariance, there are associated kinematic factors with simple angular



dependence which can be used to isolate and measure these four  $I$ 's. The following patterns, (i) and (ii), for these BR-S2SC contributions  $\tilde{I}_{\lambda_1 \lambda_2; \lambda'_1 \lambda'_2}^{g,q}$  occur identically in gluon production and in quark production:

(i)  $\theta_a$  polar-angle dependence:

The coefficients of  $\Gamma(0,0)/\Gamma(-1,-1)/\Gamma_{R,I}(0,-1)$  vary relatively as the  $W$ -decay  $d_{mm'}^1(\theta_a)$ -squared-intensity ratios

$$\begin{aligned} & \frac{1}{2} \sin^2 \theta_a / \left[ \sin^4 \frac{\theta_a}{2} \right] / \left\{ \frac{1}{\sqrt{2}} \sin \theta_a \sin^2 \frac{\theta_a}{2} \right\} \\ &= 2(1 + \cos \theta_a) / [1 - \cos \theta_a] \\ & / \left\{ \sqrt{2(1 + \cos \theta_a)(1 - \cos \theta_a)} = \sqrt{2} \sin \theta_a \right\}. \end{aligned} \quad (75)$$

(ii)  $\phi_a$  azimuthal-angle dependence in the “signal terms”:

The coefficients of  $\Gamma_R(0,-1)/\Gamma_I(0,-1)$  vary as

$$\cos \phi_a / \sin \phi_a \quad (76)$$

in each of the signal terms, i.e. as in the four-angle gluon-signal term (3) there is a factor  $\{\Gamma_R(0,-1) \cos \phi_a - \Gamma_I(0,-1) \sin \phi_a\}$ . However, in three terms there are also  $\Gamma_{R,I}(0,-1)$ 's with the opposite association of these  $\cos \phi_a$ ,  $\sin \phi_a$  factors, i.e. in a factor  $\{\Gamma_R(0,-1) \sin \phi_a + \Gamma_I(0,-1) \cos \phi_a\}$ . This opposite association occurs in half the “signal” contributions: the helicity-conserving one ( $\tilde{I}_{+-,-+}^g + \tilde{I}_{-+,-+}^g$ )<sub>sig</sub> of (54), the mixed-helicity ( $\tilde{I}_{-+,++}^g + \tilde{I}_{-+,-+}^g + \tilde{I}_{+-,-+}^g + \tilde{I}_{-+,-+}^g$ )<sub>sig</sub> of (56), and in the helicity-flip ( $\tilde{I}_{++,-+}^g + \tilde{I}_{-+,-+}^g$ )<sub>sig</sub> of (62), along with a different  $\Phi_R$  and/or  $\phi$  dependence. This different angular dependence might be used in an empirical separation of these terms from the terms with the normal  $\phi_a$  association. This different  $\Phi_R$  and/or  $\phi$  dependence is the reason that only the  $\{\Gamma_R(0,-1) \cos \phi_a - \Gamma_I(0,-1) \sin \phi_a\}$  factor appears in the signal terms in the four-angle and five-angle BR-S2SC functions.

There are analogous  $CP$ -conjugate patterns in  $\theta_b$  and  $\phi_b$  for the  $CP$ -conjugate case  $\bar{t}_2 \rightarrow W_2^- \bar{b} \rightarrow (l^- \bar{\nu}) \bar{b}$ . There is only the factor  $\{\bar{\Gamma}_R(0,1) \cos \phi_b + \bar{\Gamma}_I(0,1) \sin \phi_b\}$  in the four-angle and five-angle BR-S2SC functions. In the  $CP$ -conjugate case the patterns are also identical in gluon-production and in quark production.

### 2.5.1 Six-angle $\tilde{\mathcal{H}}_i^g$ distributions: $\phi$ dependence

To reduce the number of angles to obtain six-angle BR-S2SC functions, we integrate out either the beam-referencing azimuthal angle  $\Phi_R$  or the angle  $\phi$  between the  $t_1$  and  $\bar{t}_2$  decay planes. We only list the non-vanishing contributions. To clearly label the successive contributions, we again use the index  $i = (\lambda_1 \lambda_2, \lambda'_1 \lambda'_2)$ .

We first consider the  $t \rightarrow W^+ b \rightarrow l^+ \nu b$  channel with the  $W^-$  decaying hadronically. For

$$\tilde{\mathcal{H}}_i^g \equiv \int_0^{2\pi} d\Phi_R \tilde{I}_i^g \quad (77)$$

the non-vanishing six-angle contributions are proportional to the “background and signal parts” of the above expressions with

$$\tilde{\mathcal{H}}_i^g = 2\pi \tilde{I}_i^g. \quad (78)$$

For the helicity-conserving one,  $i = (+-, +-) + (-+, -+)$  with no  $\phi$  dependence. For the helicity-flip  $i = (++, ++)$  +  $(--, --)$  with no  $\phi$  dependence; and  $i = (++, --)$  +  $(--, ++)$  with a  $\cos \phi$  dependence in the background part, and both  $\cos \phi$  and  $\sin \phi$  dependence in the signal part. The mixed-helicity contributions vanish.

### 2.5.2 Six-angle ( $\tilde{\mathcal{H}}_i^g$ )' distributions: $\Phi_R$ dependence

If instead the  $\phi$  dependence is integrated out

$$(\tilde{\mathcal{H}}_i^g)' \equiv \int_0^{2\pi} d\phi \tilde{I}_i^g, \quad (79)$$

the non-vanishing six-angle contributions are also proportional to the above expressions:

$$(\tilde{\mathcal{H}}_i^g)' = 2\pi \tilde{I}_i^g. \quad (80)$$

For the helicity-conserving one,  $i = (+-, +-) + (-+, -+)$  with no  $\Phi_R$  dependence. For the mixed-helicity,  $i = (-+, ++)$  +  $(--, +-)$  +  $(+-, --)$  +  $(++, -+)$  with a  $\cos \Phi_R$  dependence in the background part, and both  $\cos \Phi_R$  and  $\sin \Phi_R$  dependence in the signal part. For the helicity-flip  $i = (++, ++)$  +  $(--, --)$  with no  $\Phi_R$  dependence.

### 2.5.3 Five-angle $\tilde{\mathcal{G}}_i^g$ distributions

If both the  $\Phi_R$  and  $\phi$  dependence are integrated out, the five-angle distribution  $\{\Theta_B, \theta_1^t, \theta_2^t, \theta_a, \phi_a\}$  is

$$\tilde{\mathcal{G}}_i^g \equiv \int_0^{2\pi} d\phi \int_0^{2\pi} d\Phi_R \tilde{I}_i^g. \quad (81)$$

The terms in these expressions only arise from the helicity-conserving (51) and (52), and from the helicity-flip (59) and (60):

$$\begin{aligned} \tilde{\mathcal{G}}^g|_0 &= 4\pi^2 [(\tilde{I}_{+-,+}^g + \tilde{I}_{-+,-}^g)|_0 + (\tilde{I}_{++,+}^g + \tilde{I}_{--,-}^g)|_0], \end{aligned} \quad (82)$$

$$\begin{aligned} \tilde{\mathcal{G}}^g|_{\text{sig}} &= 4\pi^2 [(\tilde{I}_{+-,+}^g + \tilde{I}_{-+,-}^g)|_{\text{sig}} + (\tilde{I}_{++,+}^g + \tilde{I}_{--,-}^g)|_{\text{sig}}]. \end{aligned} \quad (83)$$

We obtain

$$\begin{aligned} \tilde{\mathcal{G}}^g|_0 &= \frac{8\pi^3}{3} c(s, \Theta_B) \\ & \times \left\{ \frac{1}{2} \Gamma(0,0) \sin^2 \theta_a + \Gamma(-1,-1) \sin^4 \frac{\theta_a}{2} \right\} \\ & \times [\bar{\Gamma}(0,0) + \bar{\Gamma}(1,1)] \\ & \times \{ \tilde{g}_1^g(s, \Theta_B) + \mathcal{R} \tilde{g}_2^g(s, \Theta_B) \cos \theta_1^t \cos \theta_2^t \}, \end{aligned} \quad (84)$$

$$\begin{aligned} \widetilde{\mathcal{G}}^g|_{\text{sig}} = & -\frac{8\sqrt{2}\pi^3}{3} c(s, \Theta_B) \sin\theta_a \sin^2\frac{\theta_a}{2} \\ & \times \{\Gamma_R(0, -1) \cos\phi_a - \Gamma_I(0, -1) \sin\phi_a\} \\ & \times [\overline{\Gamma}(0, 0) + \overline{\Gamma}(1, 1)] \mathcal{R} \widetilde{g}_2^g(s, \Theta_B) \sin\theta_1^t \cos\theta_2^t, \end{aligned} \quad (85)$$

where the two gluon-beam-referencing factors  $\widetilde{g}_{1,2}^g(s, \Theta_B)$  are listed in (4) and (5).

Note that versus the four-angle distributions listed in the introduction, in this five-angle distribution  $\widetilde{\mathcal{G}}^g$  the gluon-beam-referencing factor  $\widetilde{g}_2^g(s, \Theta_B)$  appears in both the background and the signal contributions. For the quark-production contribution to the five-angle distribution  $\widetilde{\mathcal{G}}^g$  of (111) and (112), the analogous situation occurs in the quark-beam-referencing factors  $\widetilde{g}_{1,2}^q(s, \Theta_B)$  versus the four-angle distribution (9) and (10). Likewise for the respective  $CP$ -conjugate spin-correlation functions.

#### 2.5.4 Four-angle $\mathcal{G}_i^g$ distributions

If the  $\cos\theta_1^t$  dependence is integrated out, there is a four-angle distribution in  $\{\Theta_B, \theta_2^t, \theta_a, \phi_a\}$  with the same “ $i$ ” values as in (82) and (83),

$$\begin{aligned} \mathcal{G}_i^g & \equiv \int_{-1}^1 d(\cos\theta_1^t) \int_0^{2\pi} d\phi \int_0^{2\pi} d\Phi_R \widetilde{I}_i^g \quad (86) \\ & = \int_{-1}^1 d(\cos\theta_1^t) \widetilde{\mathcal{G}}_i^g \end{aligned}$$

which is listed in the introduction section in (2) and (3).

#### 2.5.5 Integrated BR-S2SC distributions for $CP$ -conjugate cases

For the  $CP$ -conjugate case in terms of  $\{\Phi_R, \phi, \Theta_B, \theta_2^t, \theta_1^t, \theta_b, \phi_b\}$ , the successively fewer-angle distributions similarly follow. The non-vanishing terms are proportional to the preceding “background and signal” expressions (63)–(74). The six-angle expression is

$$\widetilde{\mathcal{H}}_i^g \equiv \int_0^{2\pi} d\Phi_R \widetilde{I}_i^g = 2\pi \widetilde{I}_i^g. \quad (87)$$

For the helicity-conserving one,  $i = (+-, +-)+(-+, -+)$  with no  $\phi$  dependence. For the helicity-flip,  $i = (++, ++)+(--, --)$  with no  $\phi$  dependence; and  $i = (++, --)+(--, ++)$  with a  $\cos\phi$  dependence in the background part, and both  $\cos\phi$  and  $\sin\phi$  dependence in the signal part.

If instead the  $\phi$  dependence is integrated out, there is the six-angle expression

$$(\widetilde{\mathcal{H}}_i^g)' \equiv \int_0^{2\pi} d\phi \widetilde{I}_i^g = 2\pi \widetilde{I}_i^g \quad (88)$$

For the helicity-conserving one,  $i = (+-, +-)+(-+, -+)$  with no  $\Phi_R$  dependence. For the mixed-helicity,  $i = (-+, ++)+(--, +-)+(+-, --)+(++,-+)$  with a  $\cos\Phi_R$  dependence in the background part, and both

$\cos\Phi_R$  and  $\sin\Phi_R$  dependence in the signal part. For the helicity-flip,  $i = (++, ++)+(--, --)$  with no  $\Phi_R$  dependence.

If both the  $\Phi_R$  and  $\phi$  dependence are integrated out, the five-angle distribution  $\{\Theta_B, \theta_1^t, \theta_2^t, \theta_b, \phi_b\}$  is

$$\widetilde{\mathcal{G}}_i^g \equiv \int_0^{2\pi} d\phi \int_0^{2\pi} d\Phi_R \widetilde{I}_i^g, \quad (89)$$

and the terms in these expressions only arise from the helicity-conserving (63) and (64), and from the helicity-flip (71) and (72):

$$\begin{aligned} \widetilde{\mathcal{G}}_i^g|_0 & = 4\pi^2 [(\widetilde{I}_{+-,+}^g + \widetilde{I}_{-+,-}^g)|_0 + (\widetilde{I}_{++,++}^g + \widetilde{I}_{--,--}^g)|_0], \quad (90) \end{aligned}$$

$$\begin{aligned} \widetilde{\mathcal{G}}_i^g|_{\text{sig}} & = 4\pi^2 [(\widetilde{I}_{+-,+}^g + \widetilde{I}_{-+,-}^g)|_{\text{sig}} \\ & + (\widetilde{I}_{++,++}^g + \widetilde{I}_{--,--}^g)|_{\text{sig}}]. \quad (91) \end{aligned}$$

We obtain

$$\begin{aligned} \widetilde{\mathcal{G}}_i^g|_0 & = \frac{8\pi^3}{3} c(s, \Theta_B) \left\{ \frac{1}{2} \overline{\Gamma}(0, 0) \sin^2\theta_b + \overline{\Gamma}(1, 1) \sin^4\frac{\theta_b}{2} \right\} \\ & \times [\Gamma(0, 0) + \Gamma(-1, -1)] \\ & \times \{\widetilde{g}_1^g(s, \Theta_B) + \overline{\mathcal{R}} \widetilde{g}_2^g(s, \Theta_B) \cos\theta_1^t \cos\theta_2^t\}, \quad (92) \end{aligned}$$

$$\begin{aligned} \widetilde{\mathcal{G}}_i^g|_{\text{sig}} & = -\frac{8\sqrt{2}\pi^3}{3} c(s, \Theta_B) \sin\theta_b \sin^2\frac{\theta_b}{2} \\ & \times \{\overline{\Gamma}_R(0, 1) \cos\phi_b + \overline{\Gamma}_I(0, 1) \sin\phi_b\} \\ & \times [\Gamma(0, 0) + \Gamma(-1, -1)] \overline{\mathcal{R}} \widetilde{g}_2^g(s, \Theta_B) \cos\theta_1^t \sin\theta_2^t, \quad (93) \end{aligned}$$

where  $\widetilde{g}_{1,2}^g(s, \Theta_B)$  are given in (4) and (5).

Finally, if the  $\cos\theta_2^t$  dependence is integrated out, we obtain the four-angle distribution in  $\{\Theta_B, \theta_1^t, \theta_b, \phi_b\}$

$$\begin{aligned} \overline{\mathcal{G}}_i^g & \equiv \int_{-1}^1 d(\cos\theta_2^t) \int_0^{2\pi} d\phi \int_0^{2\pi} d\Phi_R \widetilde{I}_i^g \\ & = \int_{-1}^1 d(\cos\theta_2^t) \widetilde{\mathcal{G}}_i^g, \quad (94) \end{aligned}$$

which is listed in the introduction section in (21) and (22).

### 3 Derivation of quark-production beam-referenced stage-two spin-correlation functions

Unlike the treatment of the quark-production contribution in “I”, we do not integrate out the  $\cos\Theta_B$  dependence in this paper, as was discussed in the introduction.

### 3.1 Quark-production density matrix in JW phase convention

For comparison with the analogous gluon-density-matrix elements listed in the previous section, including the color factor, the  $t_1 \bar{t}_2$  helicity-conserving quark-production density-matrix elements in the  $(t\bar{t})_{\text{c.m.}}$  system are

$$\rho_{+-,+}^q = \rho_{-+,-}^q = \frac{g^4}{9} (1 + \cos^2 \Theta_B), \quad (95)$$

$$\rho_{-+,-}^q = \{\rho_{+-,+}^q\}^* = \frac{g^4}{9} e^{i2\Phi_B} \sin^2 \Theta_B, \quad (96)$$

with an  $e^{i2\Phi_B}$  factor in (96). These and the following density-matrix elements agree with (56) of ‘‘I’’. For  $q_1(k)q_2(n) \rightarrow t_1(p)\bar{t}_2(l)$ ,  $s = (k+n)^2 = (p+l)^2 = 4E^2$ ,  $t = (p-k)^2 = (n-l)^2 = m^2 - 2E^2(1 - \beta \cos \Theta_B)$ ,  $u = (p-n)^2 = (k-l)^2 = m^2 - 2E^2(1 + \beta \cos \Theta_B)$  where  $\beta = p/E$ . The mixed-helicity properties quark-production density-matrix elements are

$$\begin{aligned} \rho_{-+,++}^q &= \rho_{-+,-}^q = -\rho_{-+,-}^q = -\rho_{-+,-}^q \\ &= \{\rho_{-+,-}^q\}^* = \{\rho_{-+,-}^q\}^* = -\{\rho_{-+,-}^q\}^* \\ &= -\{\rho_{-+,-}^q\}^* = -\frac{2mg^4}{9s^{1/2}} e^{i\Phi_B} \sin \Theta_B \cos \Theta_B, \end{aligned} \quad (97)$$

with an overall minus sign and  $e^{i\Phi_B}$  factor. The helicity-flip quark-production density-matrix elements are

$$\rho_{-+,-}^q = \rho_{-+,-}^q = \rho_{-+,-}^q = \rho_{-+,-}^q = \frac{4m^2 g^4}{9s} \sin^2 \Theta_B. \quad (98)$$

These give the quark contributions to the BR-S2SC functions listed in Sect. 2 of ‘‘I’’, when each expression in ‘‘I’’ is multiplied by the color factor  $\frac{1}{9}$ .

### 3.2 Lepton-plus-jets channel: $\lambda_b = -1/2$ , $\lambda_{\bar{b}} = +1/2$ dominance

#### 3.2.1 $t_1 \rightarrow W_1^+ b \rightarrow (l^+ \nu) b$

With the  $i = (\lambda_1 \lambda_2, \lambda'_1 \lambda'_2)$  labelling of the present paper, the quark contributions are proportional to the ones in (98)–(109) of ‘‘I’’ as follows.

For the helicity-conserving contribution,

$$(\tilde{I}_{+-,+}^q + \tilde{I}_{-+,-}^q)|_0 = \frac{1}{9}(\tilde{I}_{++} + \tilde{I}_{--})|_0, \quad (99)$$

$$(\tilde{I}_{+-,+}^q + \tilde{I}_{-+,-}^q)|_{\text{sig}} = \frac{1}{9}(\tilde{I}_{++} + \tilde{I}_{--})|_{\text{sig}}, \quad (100)$$

$$(\tilde{I}_{+-,+}^q + \tilde{I}_{-+,-}^q)|_0 = \frac{1}{9}(\tilde{I}_{+-} + \tilde{I}_{-+})|_0, \quad (101)$$

$$(\tilde{I}_{+-,+}^q + \tilde{I}_{-+,-}^q)|_{\text{sig}} = \frac{1}{9}(\tilde{I}_{+-} + \tilde{I}_{-+})|_{\text{sig}}. \quad (102)$$

For the mixed-helicity contribution,

$$\begin{aligned} &(\tilde{I}_{-+,++}^q + \tilde{I}_{-+,-}^q + \tilde{I}_{-+,-}^q + \tilde{I}_{-+,-}^q)|_0 \\ &= \frac{1}{9}\tilde{I}^m(\varpi^+ + \bar{\eta}^-)|_0, \end{aligned} \quad (103)$$

$$\begin{aligned} &(\tilde{I}_{-+,++}^q + \tilde{I}_{-+,-}^q + \tilde{I}_{-+,-}^q + \tilde{I}_{-+,-}^q)|_{\text{sig}} \\ &= \frac{1}{9}\tilde{I}^m(\varpi^+ + \bar{\eta}^-)|_{\text{sig}}, \end{aligned} \quad (104)$$

$$\begin{aligned} &(\tilde{I}_{-+,++}^q + \tilde{I}_{-+,-}^q + \tilde{I}_{-+,-}^q + \tilde{I}_{-+,-}^q)|_0 \\ &= \frac{1}{9}\tilde{I}^m(\varpi^- + \bar{\eta}^+)|_0, \end{aligned} \quad (105)$$

$$\begin{aligned} &(\tilde{I}_{-+,++}^q + \tilde{I}_{-+,-}^q + \tilde{I}_{-+,-}^q + \tilde{I}_{-+,-}^q)|_{\text{sig}} \\ &= \frac{1}{9}\tilde{I}^m(\varpi^- + \bar{\eta}^+)|_{\text{sig}}. \end{aligned} \quad (106)$$

The helicity-flip contributions are

$$(\tilde{I}_{-+,-}^q + \tilde{I}_{-+,-}^q)|_0 = \frac{1}{9}(\tilde{I}^{m2} + \tilde{I}^{m2})|_0, \quad (107)$$

$$(\tilde{I}_{-+,-}^q + \tilde{I}_{-+,-}^q)|_{\text{sig}} = \frac{1}{9}(\tilde{I}^{m2} + \tilde{I}^{m2})|_{\text{sig}}, \quad (108)$$

$$(\tilde{I}_{-+,-}^q + \tilde{I}_{-+,-}^q)|_0 = \frac{1}{9}(\tilde{I}^{m2} + \tilde{I}^{m2})|_0, \quad (109)$$

$$(\tilde{I}_{-+,-}^q + \tilde{I}_{-+,-}^q)|_{\text{sig}} = \frac{1}{9}(\tilde{I}^{m2} + \tilde{I}^{m2})|_{\text{sig}}. \quad (110)$$

By this  $i = (\lambda_1 \lambda_2, \lambda'_1 \lambda'_2)$  labelling, the above general formulas and remarks (77)–(83) for the successively fewer-angle gluon distributions apply for the quark distributions by simply changing the superscript  $g \rightarrow q$ . Thereby, one obtains the six-angle  $\tilde{\mathcal{H}}_i^q$ ,  $(\tilde{\mathcal{H}}_i^q)'$ , and the five-angle  $\tilde{\mathcal{G}}_i^q$ .

Explicitly, in terms of  $\{\Theta_B, \theta_1^t, \theta_2^t, \theta_a, \phi_a\}$ , the five-angle distribution is

$$\begin{aligned} \tilde{\mathcal{G}}^q|_0 &= \frac{\pi^3 g^4}{27s^2} \left\{ \frac{1}{2}\Gamma(0, 0) \sin^2 \theta_a + \Gamma(-1, -1) \sin^4 \frac{\theta_a}{2} \right\} \\ &\times [\bar{\Gamma}(0, 0) + \bar{\Gamma}(1, 1)] \\ &\times \{ \tilde{g}_1^q(s, \Theta_B) + \mathcal{R} \tilde{g}_2^q(s, \Theta_B) \cos \theta_1^t \cos \theta_2^t \}, \end{aligned} \quad (111)$$

$$\begin{aligned} \tilde{\mathcal{G}}^q|_{\text{sig}} &= -\frac{\sqrt{2}\pi^3 g^4}{27s^2} \sin \theta_a \sin^2 \frac{\theta_a}{2} \\ &\times \{ \Gamma_R(0, -1) \cos \phi_a - \Gamma_I(0, -1) \sin \phi_a \} \\ &\times [\bar{\Gamma}(0, 0) + \bar{\Gamma}(1, 1)] \mathcal{R} \tilde{g}_2^q(s, \Theta_B) \sin \theta_1^t \cos \theta_2^t, \end{aligned} \quad (112)$$

where the two quark-beam-referencing factors  $\tilde{g}_{1,2}^q(s, \Theta_B)$  are listed in (11) and (12).

The simpler four-angle distribution  $\mathcal{G}_i^q = \int_{-1}^1 d(\cos \theta_1^t) \tilde{\mathcal{G}}_i^q$  is given in the introduction in (9) and (10).

3.2.2  $\bar{t}_2 \rightarrow W_2^- \bar{b} \rightarrow (l^- \bar{\nu}) \bar{b}$ 

For this  $CP$ -conjugate case, the quark contributions are proportional to (113)–(124) of “I”.

For the helicity-conserving contribution,

$$(\tilde{I}_{+-,+}^q + \tilde{I}_{-+,-}^q)|_0 = \frac{1}{9}(\tilde{I}_{++} + \tilde{I}_{--})|_0, \quad (113)$$

$$(\tilde{I}_{+-,+}^q + \tilde{I}_{-+,-}^q)|_{\text{sig}} = \frac{1}{9}(\tilde{I}_{++} + \tilde{I}_{--})|_{\text{sig}}, \quad (114)$$

$$(\tilde{I}_{+-,-}^q + \tilde{I}_{-+,+}^q)|_0 = \frac{1}{9}(\tilde{I}_{+-} + \tilde{I}_{-+})|_0, \quad (115)$$

$$(\tilde{I}_{+-,-}^q + \tilde{I}_{-+,+}^q)|_{\text{sig}} = \frac{1}{9}(\tilde{I}_{+-} + \tilde{I}_{-+})|_{\text{sig}}. \quad (116)$$

For the mixed-helicity contribution,

$$\begin{aligned} & (\tilde{I}_{-+,++}^q + \tilde{I}_{--,+-}^q + \tilde{I}_{+-,--}^q + \tilde{I}_{++,+-}^q)|_0 \\ &= \frac{1}{9} \tilde{I}^{\approx m(\bar{\omega}^+ + \bar{\eta}^-)}|_0, \end{aligned} \quad (117)$$

$$\begin{aligned} & (\tilde{I}_{-+,++}^q + \tilde{I}_{--,+-}^q + \tilde{I}_{+-,--}^q + \tilde{I}_{++,+-}^q)|_{\text{sig}} \\ &= \frac{1}{9} \tilde{I}^{\approx m(\bar{\omega}^+ + \bar{\eta}^-)}|_{\text{sig}}, \end{aligned} \quad (118)$$

$$\begin{aligned} & (\tilde{I}_{++,+-}^q + \tilde{I}_{--,+-}^q + \tilde{I}_{+-,++}^q + \tilde{I}_{-+,-}^q)|_0 \\ &= \frac{1}{9} \tilde{I}^{\approx m(\bar{\omega}^- + \bar{\eta}^+)}|_0, \end{aligned} \quad (119)$$

$$\begin{aligned} & (\tilde{I}_{++,+-}^q + \tilde{I}_{--,+-}^q + \tilde{I}_{+-,++}^q + \tilde{I}_{-+,-}^q)|_{\text{sig}} \\ &= \frac{1}{9} \tilde{I}^{\approx m(\bar{\omega}^- + \bar{\eta}^+)}|_{\text{sig}}. \end{aligned} \quad (120)$$

For the helicity-flip contribution,

$$(\tilde{I}_{++,++}^q + \tilde{I}_{--,--}^q)|_0 = \frac{1}{9}(\tilde{I}_{++}^m + \tilde{I}_{--}^m)|_0, \quad (121)$$

$$(\tilde{I}_{++,++}^q + \tilde{I}_{--,--}^q)|_{\text{sig}} = \frac{1}{9}(\tilde{I}_{++}^m + \tilde{I}_{--}^m)|_{\text{sig}}, \quad (122)$$

$$(\tilde{I}_{++,--}^q + \tilde{I}_{--,++}^q)|_0 = \frac{1}{9}(\tilde{I}_{+-}^m + \tilde{I}_{-+}^m)|_0, \quad (123)$$

$$(\tilde{I}_{++,--}^q + \tilde{I}_{--,++}^q)|_{\text{sig}} = \frac{1}{9}(\tilde{I}_{+-}^m + \tilde{I}_{-+}^m)|_{\text{sig}}. \quad (124)$$

The above general formulas and remarks in (87)–(93) for the successively fewer-angle gluon distributions apply for the quark distributions by simply changing the superscript  $g \rightarrow q$ . Thereby, one obtains the six-angle  $\tilde{\mathcal{H}}_i^q$ ,  $(\tilde{\mathcal{H}}_i^q)'$ , and the five-angle  $\tilde{\mathcal{G}}_i^q$ .

Explicitly, in terms of  $\{\Theta_B, \theta_1^t, \theta_2^t, \theta_b, \phi_b\}$ , the five-angle distribution is

$$\begin{aligned} \tilde{\mathcal{G}}^q|_0 &= \frac{\pi^3 g^4}{27 s^2} \left\{ \frac{1}{2} \bar{I}(0, 0) \sin^2 \theta_b + \bar{I}(1, 1) \sin^4 \frac{\theta_b}{2} \right\} \\ &\times [\Gamma(0, 0) + \Gamma(-1, -1)] \\ &\times \{ \tilde{g}_1^q(s, \Theta_B) + \bar{\mathcal{R}} \tilde{g}_2^q(s, \Theta_B) \cos \theta_1^t \cos \theta_2^t \}, \end{aligned} \quad (125)$$

$$\begin{aligned} \tilde{\mathcal{G}}^q|_{\text{sig}} &= -\frac{\sqrt{2} \pi^3 g^4}{27 s^2} \sin \theta_b \sin^2 \frac{\theta_b}{2} \\ &\times \{ \bar{I}_R(0, 1) \cos \phi_b + \bar{I}_I(0, 1) \sin \phi_b \} \\ &\times [\Gamma(0, 0) + \Gamma(-1, -1)] \bar{\mathcal{R}} \tilde{g}_2^q(s, \Theta_B) \cos \theta_1^t \sin \theta_2^t. \end{aligned} \quad (126)$$

The simpler four-angle distribution  $\bar{\mathcal{G}}_i^q = \int_{-1}^1 d(\cos \theta_2^t) \tilde{\mathcal{G}}_i^q$  is given in the introduction in (24) and (25).

## 4 Summary and discussion

From the top-quark beam-referenced spin-correlation function  $\mathcal{G}^{(g,q)}|_0 + \mathcal{G}^{(g,q)}|_{\text{sig}}$  with both gluon (see (2) and (3)) and quark (see (9) and (10)) production contributions, the tests for  $t_1 \rightarrow W^+ b$  decay are

(i) By measurement of  $\Gamma_R(0, -1)$ , the relative sign of the two dominant  $\lambda_b = -1/2$  helicity-amplitudes can be determined if their relative phase is  $0^\circ$  or  $180^\circ$ . Versus the partial-decay width  $\Gamma(t \rightarrow W^+ b)$ ,  $W$ -boson longitudinal–transverse interference is a large effect because in the standard model  $\eta_L \equiv \frac{\Gamma_R(0, -1)}{\Gamma} = \pm 0.46$  without/with a large  $t_R \rightarrow b_L$  chiral weak-transition-moment.

(ii) By measurement of both  $\Gamma_R(0, -1)$  and  $\Gamma_I(0, -1)$  via the  $\phi_a$  dependence, limits can be set on a possible non-trivial phase  $\beta_L \equiv \varphi_{-1, -\frac{1}{2}} - \varphi_{0, -\frac{1}{2}}$ ; see (14)–(16). Non-trivial relative phases can occur in top-quark decays if  $\tilde{T}_{FS}$  invariance is violated [1, 7]. Such a violation will occur if either (a) there is a fundamental violation of canonical time-reversal invariance, and/or (b) there are absorptive final-state interactions.

Explicit expressions for the  $A(\lambda_{W^+}, \lambda_b)$  helicity amplitudes in terms of the most general Lorentz coupling

$$W_\mu^* J_{bt}^\mu = W_\mu^* \bar{u}_b(p) \Gamma^\mu u_t(k),$$

where  $k_t = q_W + p_b$ , are given in the NKLM paper in [7]. The canonical decomposition of  $\Gamma^\mu = \Gamma^\mu_V + \Gamma^\mu_A$  is

$$\begin{aligned} \Gamma_V^\mu &= g_V \gamma^\mu + \frac{f_M}{2\Lambda_M} i\sigma^{\mu\nu} (k-p)_\nu + \frac{g_{S^-}}{2\Lambda_{S^-}} (k-p)^\mu \\ &+ \frac{g_S}{2\Lambda_S} (k+p)^\mu + \frac{g_{T^+}}{2\Lambda_{T^+}} i\sigma^{\mu\nu} (k+p)_\nu, \end{aligned}$$

$$\begin{aligned} \Gamma_A^\mu &= g_A \gamma^\mu \gamma_5 + \frac{f_E}{2\Lambda_E} i\sigma^{\mu\nu} (k-p)_\nu \gamma_5 + \frac{g_{P^-}}{2\Lambda_{P^-}} (k-p)^\mu \gamma_5 \\ &+ \frac{g_P}{2\Lambda_P} (k+p)^\mu \gamma_5 + \frac{g_{T_5^+}}{2\Lambda_{T_5^+}} i\sigma^{\mu\nu} (k+p)_\nu \gamma_5, \end{aligned}$$

where the parameters  $A_i$  are “effective-mass scales of new physics associated with the  $i$ th type additional Lorentz structure.” For a general treatment of additional Lorentz structures to pure  $(V - A)$ , the  $g_i$  or  $A_i$  must be considered as complex phenomenological parameters. Details, such as Lorentz-structure-equivalence theorems  $S \sim V + f_M$ ,  $P \sim -A + f_E, \dots$ ; the matrix elements of the divergences of these couplings; and the definitions of the chiral couplings  $g_{L,R} = g_V \mp g_A, \dots$  are in the NKLM, NC, NA papers in [7].

For  $\bar{t}_2 \rightarrow W^- \bar{b}$  decay, from the gluon (see (21) and (22)) and quark (see (24) and (25)) production contributions to the  $CP$ -conjugate BR-S2SC function for  $\overline{\mathcal{G}^{g,q}}|_0 + \overline{\mathcal{G}^{g,q}}|_{\text{sig}}$ , there are two analogous tests for  $\bar{t}_2 \rightarrow W_2^- \bar{b}$  decay. By measurement of  $\overline{T}_R(0, 1)$ , the relative sign of the two dominant helicity amplitudes  $B(0, 1/2)$  and  $B(1, 1/2)$  for  $\bar{t}_2 \rightarrow W^- \bar{b}$  can be determined if their relative phase is  $0^\circ$  or  $180^\circ$  (as in the case of large  $t_L \rightarrow \bar{b}_R$  chiral weak-transition-moment). By measurement of both  $\overline{T}_R(0, 1)$  and  $\overline{T}_1(0, 1)$  via the  $\phi_b$  dependence, limits can be set on a non-trivial phase  $\overline{\beta}_R \equiv \overline{\varphi}_{1, \frac{1}{2}} - \overline{\varphi}_{0, \frac{1}{2}}$ ; see (18)–(20).

In all these BR-S2SC functions for top-quark decay tests, the polarized-partial widths and  $W$ -boson-LT-interference widths (15) and (16) appear multiplied by the  $\theta_a$ ,  $\phi_a$  angular factors, which are expected in the helicity-formalism for the decay chain  $t_1 \rightarrow W^+ b \rightarrow (l^+ \nu) b$ . The spherical angles  $\theta_a$ ,  $\phi_a$  specify the  $l^+$  momentum in the  $W_1^+$  rest frame when there is first a boost from the  $(t\bar{t})_{\text{c.m.}}$  frame to the  $t_1$  rest frame, and then a second boost from the  $t_1$  rest frame to the  $W_1^+$  rest frame. So,  $\frac{1}{2}\Gamma(0, 0) \sin^2 \theta_a$  and  $\Gamma(-1, -1) \sin^4 \frac{\theta_a}{2}$  appear in the background terms  $\mathcal{G}^{(g,q)}|_0$ ; see (2) and (9). Similarly,  $\Gamma_R(0, -1) \sin \theta_a \sin^2 \frac{\theta_a}{2} \cos \phi_a$  and  $\Gamma_1(0, -1) \sin \theta_a \sin^2 \frac{\theta_a}{2} \sin \phi_a$  appear in the signal terms  $\mathcal{G}^{(g,q)}|_{\text{sig}}$ ; see (3) and (10). The situation is analogous for the  $\theta_b$ ,  $\phi_b$  variables in the  $CP$ -conjugate BR-S2SC functions.

The above summary is for the leading-order in QCD and the leading-order in electroweak interactions considered in this paper, assuming that the  $\lambda_b = -1/2$  and  $\lambda_{\bar{b}} = 1/2$  helicity-amplitudes dominate in  $t \rightarrow W^+ b$  decay. An important consequence of such a dominance is that the  $W$ -boson longitudinal–transverse-interference effects and BR-S2SC signatures treated in this paper are both large versus the non-dominant contributions and versus higher-order QCD and/or higher-order electroweak contributions. However, for later measurement, there are the two  $\lambda_b = 1/2$  non-dominant amplitudes in  $t_1 \rightarrow W^+ b$  decay with their two moduli and two additional relative phases. For a clear and simple “visual display” of these measurable phases, see the “ $\alpha, \beta, \gamma$ ”-relative-phases in Fig. 1 in the next to last citation in [7]. In this context, next-to-leading-order QCD, next-to-leading-order electroweak, and also  $W$ -boson and  $t$ -quark finite-width corrections require further theoretical investigation [8]. Other polarimetry techniques such as  $A_b$  polarimetry [9], and excellent understandings of detector systematics and of reaction-backgrounds will be required for a complete measurement of the four  $t \rightarrow W^+ b$  decay amplitudes and of the four decay-amplitudes for the  $CP$ -conjugate mode.

One learns a number of things from this derivation of the production density matrices and these associated BR-S2SC functions. First, the non-trivial overall minus signs and  $e^{\pm i\phi_B}$ ,  $e^{\pm i2\phi_B}$  factors appear in the same patterns in the gluon and quark production density matrices. This has the important and empirically useful consequence that most relative phase effects in these BR-S2SC functions do not depend upon whether the final  $t_1 \bar{t}_2$  system has been produced by gluon or by quark production. Therefore, as discussed in Sect. 1.1, there is a common final-state interference structure of the four-angle BR-S2SC functions, and likewise for the other additional-angle generalizations which are listed in Sects. 2 and 3. This is a common interference structure for  $W$ -boson longitudinal–transverse interference. When the  $\phi$  dependence is included, there is also a common interference-structure for  $t_1$ -quark left–right helicity interference and for  $\bar{t}_2$ -antiquark left–right helicity interference. This left–right spin-1/2 interference is in the gluon contribution, see (61) and (62), and in the quark contribution, see (109) and (110) in this paper and in (108) and (109) in “I”.

Second, for the  $t \rightarrow W^+ b$  decay mode, one learns that for a spin-correlation measurement using the “lepton + jets decay channel” to determine the relative sign of or to obtain a constraint on a possible non-trivial phase between the two dominant  $\lambda_b = -1/2$  helicity amplitudes requires use of the  $(t\bar{t})_{\text{c.m.}}$  energy of the hadronically decaying  $W$ -boson, or the kinematically equivalent cosine of the polar angle of  $W^\mp$  emission in the antitop (top) decay frame. Both this  $\cos \theta_2^*$  factor and the  $\mathcal{R} = (\text{prob } W_L) - (\text{prob } W_T)$  suppression factor appear in all the four-angle and five-angle signal terms, but not in any of the background terms. For this application of  $W$ -boson longitudinal–transverse interference, it is fortunate that in the standard model the probabilities for the presence of longitudinal/transverse  $W$ -bosons are both large. Because of this  $\mathcal{R}$  factor, it is also indeed fortunate that these probabilities are unequal,  $P(W_L) = \Gamma(0, 0)/\Gamma = 0.70$  and  $P(W_T) = \Gamma(-1, -1)/\Gamma = 0.30$ , irrespective of whether there exists a large  $t_R \rightarrow b_L$  chiral weak-transition moment.

*Acknowledgements.* This work was partially supported by U.S. Dept. of Energy Contract No. DE-FG 02-86ER40291.

## Appendix A: Spinors and their outer-products in JW phase convention

In the JW phase-convention, for application to  $t_1(p)\bar{t}_2(l)$  pair production with respective helicities  $\lambda_1$  and  $\lambda_2$ , the first particle  $p^\mu$  spinor outer-products  $u(p, \lambda_1)\bar{u}(p, \lambda_1')$ ,  $\dots$  [10–12] are

$$\begin{aligned} u(p, \pm)\bar{u}(p, \pm) &= \frac{1}{2}(\not{p} + m)(1 \pm \gamma_5 \not{\mathcal{S}}) \\ &= \frac{1}{2}(1 \pm \gamma_5 \not{\mathcal{S}})(\not{p} + m), \\ u(p, +)\bar{u}(p, -) &= \frac{1}{2}e^{i\phi}(\not{p} + m)\gamma_5 \not{\mathcal{C}} = \frac{1}{2}e^{i\phi}\gamma_5 \not{\mathcal{C}}(\not{p} + m), \end{aligned}$$

$$\begin{aligned} u(p, -)\bar{u}(p, +) &= \frac{1}{2}e^{-\iota\phi}(\not{p}+m)\gamma_5 \mathcal{C}^* \\ &= \frac{1}{2}e^{-\iota\phi}\gamma_5 \mathcal{C}^*(\not{p}+m), \end{aligned} \quad (\text{A.1})$$

with

$$p^\mu = (E; p \sin \theta \cos \phi, p \sin \theta \sin \phi, p \cos \theta), \quad p^2 = m^2,$$

$$S^\mu = \left(\frac{p}{m}; \frac{E}{m}\hat{p}\right), \quad S^2 = -1,$$

$$C^\mu = (0; \cos \theta \cos \phi - \iota \sin \phi, \cos \theta \sin \phi + \iota \cos \phi, -\sin \theta),$$

$$C \cdot C^* = -2, \quad (\text{A.2})$$

with  $\iota = \sqrt{-1}$  and where the asterisk denotes complex conjugation. The signs of  $\lambda_1$  and  $\lambda_2$  are used in labelling the spinors. Note that  $S \cdot p = 0$  and  $C \cdot p = C^* \cdot p = C \cdot S = C^* \cdot S = 0$ . For completeness, if the first particle were an antiparticle, then

$$\begin{aligned} v(p, \pm)\bar{v}(p, \pm) &= \frac{1}{2}(\not{p}-m)(1 \pm \gamma_5 \mathcal{S}) \\ &= \frac{1}{2}(1 \pm \gamma_5 \mathcal{S})(\not{p}-m), \\ v(p, +)\bar{v}(p, -) &= \frac{1}{2}e^{\iota\phi}(\not{p}-m)\gamma_5 \mathcal{C}^* = \frac{1}{2}e^{\iota\phi}\gamma_5 \mathcal{C}^*(\not{p}-m), \\ v(p, -)\bar{v}(p, +) &= \frac{1}{2}e^{-\iota\phi}(\not{p}-m)\gamma_5 \mathcal{C} = \frac{1}{2}e^{-\iota\phi}\gamma_5 \mathcal{C}(\not{p}-m). \end{aligned} \quad (\text{A.3})$$

The second antiparticle  $l^\mu$  spinor outer-products  $v(l, \lambda_2)\bar{v}(l, \lambda_2), \dots$  are

$$\begin{aligned} v(l, \pm)\bar{v}(l, \pm) &= \frac{1}{2}(\not{l}-m)(1 \pm \gamma_5 \mathcal{R}) \\ &= \frac{1}{2}(1 \pm \gamma_5 \mathcal{R})(\not{l}-m), \\ v(l, +)\bar{v}(l, -) &= \frac{1}{2}e^{-\iota\phi}(\not{l}-m)\gamma_5 \mathcal{B} = \frac{1}{2}e^{-\iota\phi}\gamma_5 \mathcal{B}(\not{l}-m), \\ v(l, -)\bar{v}(l, +) &= \frac{1}{2}e^{\iota\phi}(\not{l}-m)\gamma_5 \mathcal{B}^* = \frac{1}{2}e^{\iota\phi}\gamma_5 \mathcal{B}^*(\not{l}-m), \end{aligned} \quad (\text{A.4})$$

with

$$l^\mu = (E; -l \sin \theta \cos \phi, -l \sin \theta \sin \phi, -l \cos \theta), \quad l^2 = m^2,$$

$$R^\mu = \left(\frac{l}{m}; -\frac{E}{m}\hat{l}\right), \quad R^2 = -1,$$

$$B^\mu = (0; \cos \theta \cos \phi - \iota \sin \phi, \cos \theta \sin \phi + \iota \cos \phi, -\sin \theta),$$

$$B \cdot B^* = -2, \quad (\text{A.5})$$

so  $R \cdot l = 0$  and  $B \cdot l = B^* \cdot l = B \cdot R = B^* \cdot R = 0$ . In the  $(t_1 \bar{t}_2)_{\text{c.m.}}$  system, where the  $\bar{t}_2(l)$  is back-to-back with the  $t_1(p)$ ,  $C \cdot l = C^* \cdot l = C \cdot R = C^* \cdot R = 0$ . In this system,  $B^\mu$  and  $C^\mu$  are identical but in calculating, it is sometimes useful to keep them distinct. For completeness, if  $l^\mu$  were a

particle then

$$\begin{aligned} u(l, \pm)\bar{u}(l, \pm) &= \frac{1}{2}(\not{l}+m)(1 \pm \gamma_5 \mathcal{R}) \\ &= \frac{1}{2}(1 \pm \gamma_5 \mathcal{R})(\not{l}+m), \\ u(l, +)\bar{u}(l, -) &= \frac{1}{2}e^{-\iota\phi}(\not{l}+m)\gamma_5 \mathcal{B} = \frac{1}{2}e^{-\iota\phi}\gamma_5 \mathcal{B}(\not{l}+m), \\ u(l, -)\bar{u}(l, +) &= \frac{1}{2}e^{\iota\phi}(\not{l}+m)\gamma_5 \mathcal{B}^* = \frac{1}{2}e^{\iota\phi}\gamma_5 \mathcal{B}^*(\not{l}+m). \end{aligned} \quad (\text{A.6})$$

These outer-products follow from the following spinors:  $u(p, \lambda)|_\phi, v(p, \lambda)|_\phi, \dots$ , constructed following the procedure of [12]. The sub-label  $\phi$  on these spinors denotes the non-zero value of the third Euler angle in the Wigner  $D$  function; see discussion below. This sub-label is normally suppressed because it is apparent from the context. For the first particle  $p^\mu$ ,

$$\begin{aligned} u(p, +) &= \frac{1}{\sqrt{E+m}}(\not{p}+m) \begin{bmatrix} \cos \frac{\theta}{2} \\ e^{i\phi} \sin \frac{\theta}{2} \\ 0 \\ 0 \end{bmatrix} \\ &= \sqrt{E+m} \begin{bmatrix} \cos \frac{\theta}{2} \\ e^{i\phi} \sin \frac{\theta}{2} \\ \frac{p}{E+m} \begin{bmatrix} \cos \frac{\theta}{2} \\ e^{i\phi} \sin \frac{\theta}{2} \end{bmatrix} \end{bmatrix}, \\ u(p, -) &= \frac{1}{\sqrt{E+m}}(\not{p}+m) \begin{bmatrix} -e^{-i\phi} \sin \frac{\theta}{2} \\ \cos \frac{\theta}{2} \\ 0 \\ 0 \end{bmatrix} \\ &= \sqrt{E+m} \begin{bmatrix} -e^{-i\phi} \sin \frac{\theta}{2} \\ \cos \frac{\theta}{2} \\ \frac{p}{E+m} \begin{bmatrix} e^{-i\phi} \sin \frac{\theta}{2} \\ -\cos \frac{\theta}{2} \end{bmatrix} \end{bmatrix}, \\ v(p, +) &= -\frac{1}{\sqrt{E+m}}(\not{p}-m) \begin{bmatrix} 0 \\ 0 \\ \sin \frac{\theta}{2} \\ -e^{i\phi} \cos \frac{\theta}{2} \end{bmatrix} \\ &= -\sqrt{E+m} \begin{bmatrix} \frac{p}{E+m} \begin{bmatrix} -\sin \frac{\theta}{2} \\ e^{i\phi} \cos \frac{\theta}{2} \end{bmatrix} \\ \sin \frac{\theta}{2} \\ -e^{i\phi} \cos \frac{\theta}{2} \end{bmatrix}, \\ v(p, -) &= -\frac{1}{\sqrt{E+m}}(\not{p}-m) \begin{bmatrix} 0 \\ 0 \\ e^{-i\phi} \cos \frac{\theta}{2} \\ \sin \frac{\theta}{2} \end{bmatrix} \\ &= -\sqrt{E+m} \begin{bmatrix} \frac{p}{E+m} \begin{bmatrix} e^{-i\phi} \cos \frac{\theta}{2} \\ \sin \frac{\theta}{2} \end{bmatrix} \\ e^{-i\phi} \cos \frac{\theta}{2} \\ \sin \frac{\theta}{2} \end{bmatrix}. \end{aligned} \quad (\text{A.7})$$

For the second particle specified by  $l^\mu$  of (A.5), the spinors are

$$\begin{aligned}
 u(l, -) &= \frac{1}{\sqrt{E+m}} (\not{l} + m) \begin{bmatrix} \cos \frac{\theta}{2} \\ e^{i\phi} \sin \frac{\theta}{2} \\ 0 \\ 0 \end{bmatrix} \\
 &= \sqrt{E+m} \begin{bmatrix} \cos \frac{\theta}{2} \\ e^{i\phi} \sin \frac{\theta}{2} \\ -\frac{l}{E+m} \begin{bmatrix} \cos \frac{\theta}{2} \\ e^{i\phi} \sin \frac{\theta}{2} \end{bmatrix} \end{bmatrix}, \\
 u(l, +) &= \frac{1}{\sqrt{E+m}} (\not{l} + m) \begin{bmatrix} -e^{-i\phi} \sin \frac{\theta}{2} \\ \cos \frac{\theta}{2} \\ 0 \\ 0 \end{bmatrix} \\
 &= \sqrt{E+m} \begin{bmatrix} -e^{-i\phi} \sin \frac{\theta}{2} \\ \cos \frac{\theta}{2} \\ \frac{l}{E+m} \begin{bmatrix} -e^{-i\phi} \sin \frac{\theta}{2} \\ \cos \frac{\theta}{2} \end{bmatrix} \end{bmatrix}, \\
 v(l, -) &= -\frac{1}{\sqrt{E+m}} (\not{l} - m) \begin{bmatrix} 0 \\ 0 \\ \sin \frac{\theta}{2} \\ -e^{i\phi} \cos \frac{\theta}{2} \end{bmatrix} \\
 &= -\sqrt{E+m} \begin{bmatrix} \frac{l}{E+m} \begin{bmatrix} \sin \frac{\theta}{2} \\ -e^{i\phi} \cos \frac{\theta}{2} \end{bmatrix} \\ \sin \frac{\theta}{2} \\ -e^{i\phi} \cos \frac{\theta}{2} \end{bmatrix}, \\
 v(l, +) &= -\frac{1}{\sqrt{E+m}} (\not{l} - m) \begin{bmatrix} 0 \\ 0 \\ e^{-i\phi} \cos \frac{\theta}{2} \\ \sin \frac{\theta}{2} \end{bmatrix} \\
 &= -\sqrt{E+m} \begin{bmatrix} -\frac{l}{E+m} \begin{bmatrix} e^{-i\phi} \cos \frac{\theta}{2} \\ \sin \frac{\theta}{2} \end{bmatrix} \\ e^{-i\phi} \cos \frac{\theta}{2} \\ \sin \frac{\theta}{2} \end{bmatrix}. \quad (\text{A.8})
 \end{aligned}$$

A useful alternative spinor-construction is to set the third Euler angle to zero. When needed for clarity, we denote this alternate spinor-construction by the sub-label “0”. The formulas for these  $u(p, \lambda)|_0$  and  $v(p, \lambda)|_0$  spinors are proportional to those listed above. Explicitly, for  $p^\mu$ ,

$$u(p, \pm)|_0 = e^{\mp i\phi/2} u(p, \pm)|_\phi, \quad v(p, \pm)|_0 = e^{\mp i\phi/2} v(p, \pm)|_\phi, \quad (\text{A.9})$$

and for  $l^\mu$ ,

$$u(l, \pm)|_0 = e^{\pm i\phi/2} u(l, \pm)|_\phi, \quad v(l, \pm)|_0 = e^{\pm i\phi/2} v(l, \pm)|_\phi. \quad (\text{A.10})$$

Consequently, the  $e^{\pm i\phi}$  factors are absent in their associated outer-products, so in place of the above outer-products we have  $u(p, +)|_0 \bar{u}(p, -)|_0 = \frac{1}{2}(\not{p} + m)\gamma_5 \mathcal{C}, \dots$

Similarly, in place of the spin-one particle  $\epsilon^\mu(p, \lambda)|_\phi$  polarization vectors in [11],

$$\epsilon^\mu(p, \lambda)|_0 = e^{-i\lambda\phi} \epsilon^\mu(p, \lambda)|_\phi; \quad \lambda = \pm 1, 0 \quad (\text{A.11})$$

The  $P$  parity and  $T$  time-reversal discrete symmetry properties for the above spinors do not depend on the choice of the third Euler angle. With  $P = \gamma^0$  and  $\lambda = \pm$

$$Pu(p, \lambda) = u(l, -\lambda),$$

$$Pv(p, \lambda) = -v(l, -\lambda),$$

where  $l = |\vec{l}| = p = |\vec{p}|$ . In these and the following relations, the  $p$  denotes the  $u(p, \lambda)|_\phi$  spinor which is listed in (A.7) and the  $l$  denotes the  $u(l, \lambda)|_\phi$  spinor which is listed in (A.8), etc. The gamma matrices are in the Dirac representation, which is sometimes named the “standard” or “Dirac–Pauli” [12] representation. With  $T = i\gamma^2\gamma^5\gamma^0 = \gamma^1\gamma^3$ ,

$$Tu^*(p, \pm) = \mp u(l, \pm),$$

$$Tv^*(p, \pm) = \mp v(l, \pm),$$

where  $l = |\vec{l}| = p = |\vec{p}|$ , and the asterisk denotes complex conjugation.

The  $C$  charge-conjugation discrete symmetry properties do depend on the choice of the third Euler angle. With  $C = i\gamma^2\gamma^0$ , for the first particle  $p^\mu$  spinors (see (A.7))

$$v(p, \pm)|_\phi = e^{\pm i\phi} i\gamma^2 u^*(p, \pm)|_\phi = e^{\pm i\phi} C\bar{u}^T(p, \pm)|_\phi,$$

$$u(p, \pm)|_\phi = e^{\pm i\phi} i\gamma^2 v^*(p, \pm)|_\phi,$$

and for the second particle  $l^\mu$  spinors (see (A.8))

$$v(l, \pm)|_\phi = e^{\mp i\phi} i\gamma^2 u^*(l, \pm)|_\phi = e^{\mp i\phi} C\bar{u}^T(l, \pm)|_\phi,$$

$$u(l, \pm)|_\phi = e^{\mp i\phi} i\gamma^2 v^*(l, \pm)|_\phi.$$

The  $C$  relations for the  $u(p, \pm)|_0$  and  $v(p, \pm)|_0$  spinors are obtained by omitting the  $e^{\pm i\phi}$  factors in these equations.

In the gluon (quark) production density matrices used in the text, we follow the  $u(p, \lambda)|_\phi, v(p, \lambda)|_\phi$  choice which corresponds to the choice made in “I” to use a non-zero third Euler angle in describing  $t_1\bar{t}_2$  pair production in the helicity-formalism. Following the Jacob–Wick papers [5], this non-zero choice of the third argument in the various Wigner  $D$  functions is more often chosen in the literature on applications of the helicity-formalism. An important exception occurs in treating sequential decay chains. For instance, in “I” for describing the sequential-decay matrix  $R_{\lambda_1\lambda'_1}$  for  $t \rightarrow W^+b \rightarrow (l^+\nu)b$  in “I”, we do set the third Euler angle equal to zero. For specifying the second-stage axes orientation for  $W^+ \rightarrow l^+\nu$  versus the first-stage axes from  $t \rightarrow W^+b$  where the  $W^+$  momentum is in the  $D$  functions, it is conceptually simpler not to make an unnecessary additional rotation about the  $W^+$  axis in the first-stage  $D$  functions; see Sect. II of [13]. For  $t \rightarrow W^+b$  decay, unlike in completely orienting a rigid body in classical mechanics, it

is only necessary to correctly orient the  $\theta_1^t, \phi_1^t$  direction of the  $W^+$  momentum. This only involves the first two Euler angles. Unlike for specifying the  $W^+$  momentum, in the case of orienting a rigid body, a third Euler angle rotation is required, for one must also specify the amount of angular rotation of the non-cylindrically-symmetric rigid body about its  $\theta_1^t, \phi_1^t$  axis.

Obviously, some care is needed to insure that the choice of spinors corresponds to the choice of third argument used in the  $D$  functions in the helicity-formalism. This occasionally needs emphasis because it is common to use the  $u(p, \lambda)|_0$  and  $v(p, \lambda)|_0$  type spinors, and also common to use non-zero third-argument  $D$  functions in the helicity-formalism. If used simultaneously to describe the same elementary particle reaction, this would be an inconsistent treatment of relative-phase effects.

For both helicity choices, these spinors were checked by using them to calculate decay matrix elements and comparing their overall signs and  $\theta, \phi$  dependence with those of the helicity-formalism: Using the spinors for the final neutrinos/antineutrinos, the first particle  $p^\mu$  spinors were checked for  $\tau^- \rightarrow \nu\pi^-, \tau^+ \rightarrow \bar{\nu}\pi^+$  and the second particle  $l^\mu$  spinors were checked for  $\tau^- \rightarrow \pi^-\nu, \tau^+ \rightarrow \pi^+\bar{\nu}$ . They were checked for  $Z^0 \rightarrow \tau^-\tau^+$  and  $Z^0 \rightarrow \tau^+\tau^-$ . The quark-production density-matrix elements for  $q_1\bar{q}_2 \rightarrow t_1\bar{t}_2$  were calculated as in Appendix B and agree with (56) of “I”.

## Appendix B: Derivation of gluon-production density-matrix elements in JW phase convention

For the gluon-production sequence  $g_1g_2 \rightarrow t_1\bar{t}_2$ , the density-matrix elements are

$$\begin{aligned} & \rho_{\lambda_1\lambda_2, \lambda'_1\lambda'_2}^g(\Theta_B, \Phi_B) \\ &= \frac{1}{4} \sum_{s_1, s_2} \mathcal{M}(s_1s_2, \lambda_1\lambda_2) \mathcal{M}^*(s_1s_2, \lambda'_1\lambda'_2) \end{aligned} \quad (\text{B.1})$$

for the QCD Lorentz-invariant amplitude  $\mathcal{M}$  to the leading-order in  $\alpha_s$ . The initial gluon spin-averaging is over the massless  $g_1$  and  $g_2$  helicities  $s_1, s_2$ . The  $t_1$  and  $\bar{t}_2$  helicities in the amplitude are  $\lambda_1, \lambda_2$ . In the complex-conjugate amplitude,  $\lambda'_1, \lambda'_2$  are their helicities. For simplicity, the initial color-averaging, the final color summation, and the associated color indices are not displayed explicitly in (B.1). With the spinor outer-products of Appendix A, from (B.1) by normal tracing techniques, the expressions given in the text follow for  $\rho_{\lambda_1\lambda_2, \lambda'_1\lambda'_2}^g$  and analogously for  $\rho_{\lambda_1\lambda_2, \lambda'_1\lambda'_2}^g$ ; compare Appendix A of [14]. Similarly, for the  $\Theta_t, \Phi_t$  beam coordinate system of Fig. 3, the alternative  $\tilde{\rho}_{\lambda_1\lambda_2, \lambda'_1\lambda'_2}^g$  gluon production density-matrix elements of Appendix C follow. For either beam coordinate system, there are 5 distinct gluon-production density-matrix elements and 5 distinct quark-production density-matrix elements. The other density-matrix elements follow either by hermiticity

or by the  $P$  and  $C$  discrete symmetries which are present in the outer-products and in the QCD Feynman-rules.

## Appendix C: $\Theta_t, \Phi_t$ production density-matrix elements in JW phase convention

As shown in Fig. 3, the alternative  $\Theta_t, \Phi_t$  beam-referenced production density-matrices  $\tilde{\rho}_{\lambda_1\lambda_2, \lambda'_1\lambda'_2}$  are for a beam coordinate system  $(x_b, y_b, z_b)$  in the  $(t\bar{t})_{\text{c.m.}}$  frame in which the  $g_1$  gluon-momentum or  $q_1$  quark-momentum “beam” direction defines the positive  $z_b$  axis. The final  $t_1$  momentum is specified by the spherical angles  $\Theta_t, \Phi_t$ . In this appendix, we denote these alternative density-matrix elements by a “tilde”.

We do not use these alternative density-matrix elements in the derivation of the BR-S2SC’s because the azimuthal angle  $\Phi_t$  is specified versus the initial-beam direction, whereas in  $\rho_{\lambda_1\lambda_2, \lambda'_1\lambda'_2}$  derived in Appendix B and used in the text, the azimuthal angle  $\Phi_B$  is defined versus the final  $t_1$  momentum direction in the  $(t\bar{t})_{\text{c.m.}}$ . In using the helicity-formalism for BR-S2SC functions for two-body pair production such as  $t_1\bar{t}_2$ , the final  $t_1$  momentum direction is the natural/most-convenient axis [14] for analyzing the two sequential-decay-chain-processes and, therefore, for simultaneously incorporating the beam-referencing.

In the JW phase convention, the gluon-production density-matrix elements are

$$\tilde{\rho}_{+-, +-}^g = \tilde{\rho}_{-+, -+}^g = \tilde{c}(s, \Theta_t) \frac{4p^2}{s} \sin^2 \Theta_t (1 + \cos^2 \Theta_t), \quad (\text{C.1})$$

$$\tilde{\rho}_{-+, +-}^g = \{\tilde{\rho}_{+-, -+}^g\}^* = \tilde{c}(s, \Theta_t) \frac{4p^2}{s} e^{i2\Phi_t} \sin^4 \Theta_t, \quad (\text{C.2})$$

$$\tilde{\rho}_{-+, ++}^g = \tilde{\rho}_{-+, --}^g = -\tilde{\rho}_{--, +-}^g = -\tilde{\rho}_{++, +-}^g \quad (\text{C.3})$$

$$\begin{aligned} &= \{\tilde{\rho}_{++, -+}^g\}^* = \{\tilde{\rho}_{--, -+}^g\}^* \\ &= -\{\tilde{\rho}_{+-, --}^g\}^* = -\{\tilde{\rho}_{+-, ++}^g\}^* \end{aligned} \quad (\text{C.4})$$

$$= \tilde{c}(s, \Theta_t) \frac{8p^2 m}{s^{3/2}} e^{i\Phi_t} \sin^3 \Theta_t \cos \Theta_t, \quad (\text{C.5})$$

$$\begin{aligned} \tilde{\rho}_{++, ++}^g &= \tilde{\rho}_{--, --}^g \\ &= \tilde{c}(s, \Theta_t) \frac{4m^2}{s} \left( 1 + \frac{4p^2}{s} [1 + \sin^4 \Theta_t] \right), \end{aligned} \quad (\text{C.6})$$

$$\begin{aligned} \tilde{\rho}_{++, --}^g &= \tilde{\rho}_{--, ++}^g \\ &= \tilde{c}(s, \Theta_t) \frac{4m^2}{s} \left( 1 - \frac{4p^2}{s} [1 + \sin^4 \Theta_t] \right), \end{aligned} \quad (\text{C.7})$$

where

$$\tilde{c}(s, \Theta_t) = \frac{s^2 g^4}{96(m^2 - t)^2 (m^2 - u)^2} \left[ 7 + \frac{36p^2}{s} \cos^2 \Theta_t \right]. \quad (\text{C.8})$$



Note that there is not an overall minus sign in (C.5) versus (32) in the text. These  $\tilde{\rho}_{\lambda_1\lambda_2;\lambda'_1\lambda'_2}$  were derived using the  $u(p, \pm)|_0, \dots$  spinor outer-products of Appendix A; see the remarks after (A.2). These gluon-production density-matrix elements (C.1)–(C.7) agree in magnitude with

$$\frac{1}{4} \sum_{h_{g1}, h_{g2}} (h_{g1}, h_{g2}, \lambda_1, \lambda_2)(h_{g1}, h_{g2}, \lambda'_1, \lambda'_2)^* \quad (\text{C.9})$$

constructed from (A.2) of reference [15]. The  $e^{\pm i2\Phi_t}$ ,  $e^{\pm i\Phi_t}$  factors are missing in (C.9) and some overall signs differ between (C.1)–(C.7) and (C.9).

From the derivation of  $\tilde{\rho}_{\lambda_1\lambda_2;\lambda'_1\lambda'_2}^q$ , one obtains a simple “Substitution Rule” for obtaining these  $\Theta_t$ ,  $\Phi_t$  density-matrix elements from the  $\Theta_B$ ,  $\Phi_B$  ones in the text:

$$\begin{aligned} \{\cos \Theta_B &\rightarrow \cos \Theta_t; \\ e^{i\Phi_B} &\rightarrow 1; \\ \sin \Theta_B &\rightarrow -e^{i\Phi_t} \sin \Theta_t \end{aligned}$$

in “ $\lambda_1, \lambda_2 = -, +$ ” and “ $\lambda'_1, \lambda'_2 = +, -$ ”, with complex-conjugation of this rule for “ $-$ ”  $\leftrightarrow$  “ $+$ ” cases.}

This latter step in the substitution rule, which involves a minus sign, occurs due to the sine functions which arise from  $q \cdot C, q \cdot B, \dots$  factors in the spinor outer-products. This latter step needs to be performed twice in some of the helicity-conserving density-matrix elements, and once in the mixed-helicity density-matrix elements.

The quark-production density-matrix elements are

$$\tilde{\rho}_{+-,+}^q = \tilde{\rho}_{-+,-}^q = \frac{g^4}{9} (1 + \cos^2 \Theta_t) \quad (\text{C.10})$$

$$\tilde{\rho}_{-+,-}^q = \{\tilde{\rho}_{+-,+}^q\}^* = \frac{g^4}{9} e^{i2\Phi_t} \sin^2 \Theta_t \quad (\text{C.11})$$

$$\begin{aligned} \tilde{\rho}_{-+,++}^q &= \tilde{\rho}_{-+,-}^q = -\tilde{\rho}_{-+,-}^q = -\tilde{\rho}_{-+,-}^q \\ &= \{\tilde{\rho}_{-+,-}^q\}^* = \{\tilde{\rho}_{-+,-}^q\}^* = -\{\tilde{\rho}_{-+,-}^q\}^* \\ &= -\{\tilde{\rho}_{-+,-}^q\}^* = \frac{2mg^4}{9s^{1/2}} e^{i\Phi_t} \sin \Theta_t \cos \Theta_t, \end{aligned} \quad (\text{C.12})$$

$$\tilde{\rho}_{+,++}^q = \tilde{\rho}_{-,-}^q = \tilde{\rho}_{+,--}^q = \tilde{\rho}_{-,-,++}^q = \frac{4m^2g^4}{9s} \sin^2 \Theta_t. \quad (\text{C.13})$$

There is not an overall minus sign in (C.12) versus (97) in the text. The above substitution rule also yields these  $\tilde{\rho}_{\lambda_1\lambda_2;\lambda'_1\lambda'_2}^q$  density-matrix elements from the  $\rho_{\lambda_1\lambda_2;\lambda'_1\lambda'_2}^q$  ones in the text.

## References

1. C.A. Nelson, E.G. Barbagiovanni, J.J. Berger, E.K. Putschel, J.R. Wickman, Eur. Phys. J. C **45**, 121 (2006); hep-ph/0506240. This paper is referred to as “I”. In the present paper,  $g$  and  $q$  superscripts are used to distinguish
- the gluon and quark production contributions to physical quantities. Subscripts  $i = (\lambda_1\lambda_2, \lambda'_1\lambda'_2)$ , with  $\lambda_1\lambda_2, \lambda'_1\lambda'_2$  the signs of the  $t_1, t_2$  helicities, are used to label  $(t\bar{t})_{c.m.}$  production density-matrix elements  $\rho_{\lambda_1\lambda_2,\lambda'_1\lambda'_2}(\Theta_B, \Phi_B)$  and their associated contributions to beam-referenced stage-two spin-correlation functions (BR-S2SC)
2. F. Abe et al. (CDF collaboration), Phys. Rev. Lett. **74**, 2626 (1995); S. Abachi et. al. (D0 collaboration), ibid. **74**, 2632 (1995)
3. D. Acosta et al. (CDF-collaboration), Phys. Rev. D **71**, 031101 (2005); V.M. Abazov et al. (D0-collaboration), Phys. Lett. B **617**, 1 (2005); F. Fiedler, hep-ex/0506005.
4. ATLAS Technical Proposal, CERN/LHCC/94-43, LHCC/P2 (1994); CMS Technical Design Report, CERN-LHCC-97-32; CMS-TDR-3 (1997). For  $1\text{fb}^{-1}$  to tape, there will be  $\sim 10^5$  events for  $t\bar{t} \rightarrow \mu\nu X$ , see F. Gianotti, GGI Inaugural Conf., Arcetri (2005)
5. M. Jacob, G. Wick, Ann. Phys. (NY) **7**, 209 (1959); K.-C. Chou, JETP **36**, 909 (1959); M.I. Shirokov, ibid. **39**, 633 (1960). The Jacob–Wick phase convention includes the phase convention of Rose for the  $d$  functions; M.E. Rose, Elementary Theory of Angular Momentum (Wiley, New York 1957)
6. In the standard model, for the  $t \rightarrow W^+ b$  decay mode, the relative phase is  $0^\circ$  between the dominant  $A(0, -1/2)$  and  $A(-1, -1/2)$  helicity amplitudes. However, as a consequence of Lorentz invariance, the four intensity ratios,  $\Gamma_{L,T}|\lambda_b=\mp\frac{1}{2}|/\Gamma(t \rightarrow W^+ b)$  for the SM’s ( $V-A$ ) coupling are identical to those which occur in the case of an additional chiral-tensorial coupling of relative strength  $\Lambda_+ = E_W/2 \sim 53\text{ GeV}$  in  $g_L = g_{f_M+f_E} = 1$  units;  $\frac{1}{2}\Gamma^\mu = g_L\gamma^\mu P_L + \frac{g_{f_M+f_E}}{2\Lambda_+}i\sigma^{\mu\nu}(k_t - p_b)_\nu P_R = P_R(\gamma^\mu + i\sigma^{\mu\nu}v_\nu)$  where  $v^\nu = q_W^\nu/E_W$ ,  $P_{L,R} = \frac{1}{2}(1 \mp \gamma_5)$ . In the case of such an additional large  $t_R \rightarrow b_L$  chiral weak-transition moment, there is instead a  $180^\circ$  relative phase between the  $A(0, -1/2)$  and  $A(-1, -1/2)$  helicity amplitudes; see C.A. Nelson, Phys. Rev. D **65**, 074033 (2002); in Physics at Extreme Energies, edited by N. van Hieu and J.T.T. Van (Gioi Publishers, Vietnam, 2001), p. 369; in Results and Perspectives in Particle Physics, edited by M. Greco (INFN, Frascati, Roma, Italy, 2003), p. 319; hep-ph/0411072 and references therein
7. C.A. Nelson, Phys. Rev. D **41**, 2805 (1990); in Results and Perspectives in Particle Physics, edited by M. Greco (Editions Frontierses, Gif-sur-Yvette, France 1994), p. 259; C.A. Nelson, B.T. Kress, M. Lopes, T.P. McCauley, Phys. Rev. D **56**, 5928 (1997); ibid. D **57**, 5923 (1998); C.A. Nelson, A.M. Cohen, Eur. Phys. J. C **8**, 393 (1999); C.A. Nelson, L.J. Adler, Eur. Phys. J. C **17**, 399(2000)
8. Next-to-leading-order QCD corrections: W. Bernreuther, A. Brandenburg, Z.G. Si, P. Uwer, Nucl. Phys. **690**, 81 (2004); hep-ph/0410197; W. Bernreuther, M. Fuecker, Z.G. Si, hep-ph/0508091 and references therein; Electroweak corrections: J.H. Kuhn, A. Scharf, P. Uwer, hep-ph/0508092; Finite decay-width effects: N. Kauer, D. Zeppenfeld, Phys. Rev. D **65**, 014021(2002); H.S. Do, S. Groote, J.G. Korner, M.C. Mauser, ibid. **67**, 091501 (2003); and N. Kauer, ibid. **67**, 054031 (2003)
9. C.A. Nelson, Eur. Phys. J. C **19**, 323 (2001)
10. V. Barger, J. Ohnemus, R.J.N. Phillips, Phys. Rev. D **35**, 166 (1987)
11. P.R. Auvil, J.J. Brehm, Phys. Rev. **145**, 1152 (1966)

12. J.J. Sakurai, *Advanced Quantum Mechanics* (Addison-Wesley, Reading, MA 1967) p. 194–199
13. C.A. Nelson et al., *Phys. Rev. D* **50**, 4544 (1994)
14. C.A. Nelson, *Phys. Rev. D* **43**, 1465 (1991)
15. G.L. Kane, G.A. Landinsky, C.P. Yuan, *Phys. Rev. D* **45**, 124 (1992)